DRAFT BRIDGE HYDRAULIC REPORT

Florida Department of Transportation

District One

S.R. 789 (Longboat Key) PD&E Study

Limits of Project: From North Shore Road to Coquina Park Entrance

Manatee County, Florida

Financial Management Number: 436676-1-22-01

ETDM Number: 14382

Date: July 2022

The environmental review, consultation, and other actions required by applicable federal environmental laws for this project are being, or have been, carried out by the Florida Department of Transportation (FDOT) pursuant to 23 U.S.C. § 327 and a Memorandum of Understanding dated May 26, 2022 and executed by the Federal Highway Administration and FDOT.

BRIDGE HYDRAULICS REPORT
FOR S.R. 789 (GULF OF MEXICO DRIVE) OVER LONGBOAT PASS
IN MANATEE COUNTY

FOR
FLORIDA DEPARTMENT OF TRANSPORTATION DISTRICT 1
FINANCIAL PROJECT ID: 436676-1-22-01

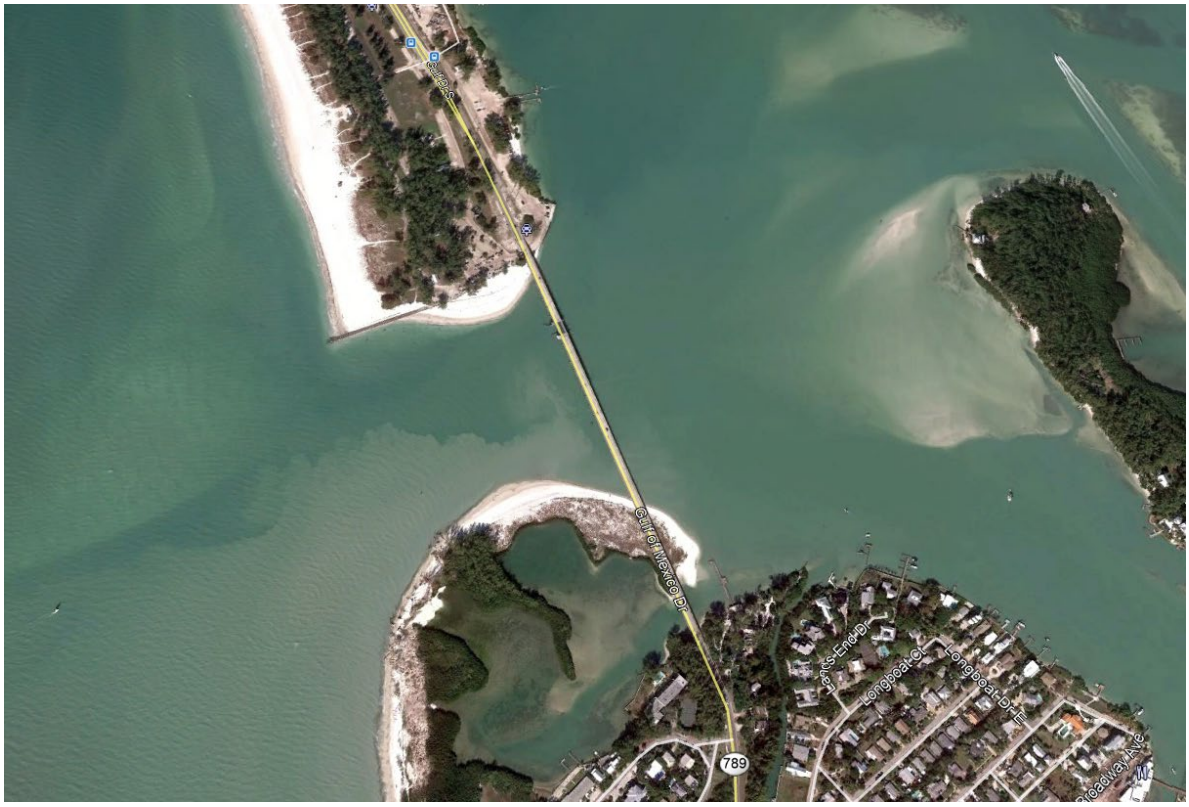

PREPARED FOR:
SCALAR CONSULTING GROUP
13337 NORTH 56TH STREET
TAMPA, FL 33617

PREPARED BY:
INTERA INCORPORATED
CERTIFICATE OF AUTHORIZATION NUMBER 00009062
2114 NW 40TH TERRACE, SUITE A-1
GAINESVILLE, FL 32605
FEBRUARY 6, 2026

Project Index and Engineer's Certification

I. Project Information

S.R. 789 (Gulf of Mexico Drive) over Longboat Pass

II. Governing Standards and Specifications

a) FDOT Drainage Design Guide (2023)
b) FDOT Drainage Manual (January 2023)
c) FDOT Design Manual (January 2023)

III. Computer Programs used for Calculations and Analysis

a) ADCIRC Version 51.52
b) SWAN Version 41.61
c) Microsoft Office Excel 2016

The official record of this report is the electronic file digitally signed and sealed under 61G15-23.004, F.A.C.

I, Miao Tian, Ph.D., P.E., hereby state that this report, as listed in the following Table of Contents, is, to the best of my knowledge and belief, true and correct and represents the described work in accordance with current established engineering practices. I hereby certify that I am a Licensed Professional Engineer in the State of Florida practicing with INTERA Incorporated, and that I have supervised the preparation of and approve the evaluations, findings, opinions and conclusions hereby reported.

This document has been digitally signed and sealed by Miao Tian, Ph.D., P.E. on 2/6/2026 using a Digital Signature.

Printed copies of this document are not considered signed and sealed and the signature must be verified on any electronic copies.

INTERA Incorporated
2114 NW 40th Terrace, Suite A-1
Gainesville, FL 32605
Phone (352) 681-4833
Certificate of Authorization No. 9062
Miao Tian, Ph.D., P.E.
Florida P.E. #86557

Table of Contents

List of Figures

List of Tables

Executive Summary

FDOT District 1 is evaluating the proposed replacement of the Gulf of Mexico Drive (S.R. 789) Bridge over Longboat Pass, located within Manatee County. As part of the PD&E (Project Development and Environment) study, Scalar Consulting Group (Scalar) has contracted INTERA Incorporated (INTERA) to perform a bridge hydraulic analysis for the replacement bridge. Three design alternatives were evaluated. Design hydraulic conditions at the bridge are controlled by hurricane storm surge. Table ES. 1 summarizes peak storm surge conditions at the bridge. Table ES. 2 through Table ES. 4 summarize design scour conditions at the bridge.

Table ES. 1 Summary of Hydraulic Conditions

	Design (50-Year) Flood	Base (100-Year) Flood	Greatest (500-Year) Flood
Stage Elevation w/o SLR (ft-NAVD88)	+7.6	+8.9	+11.8
Stage Elevation w/ SLR (ft-NAVD88)	+9.1	+10.3	+13.3
Discharge w/o SLR (cfs)	218,319	227,383	220,318
Velocity w/o SLR (ft/s)	10.8	10.9	11.4
Exceedance Probability (%)	2	1	0.2
Frequency (yr)	50	100	500

Table ES. 2 100-Year Design Scour Conditions for Alternative 1

Bent	Initial Bed Elevation (ft-NAVD88)	Degradation (ft)	Contraction Scour (ft)	Local Scour (ft)	Total Scour (ft)	Final Bed Elevation (ft-NAVD88)
2-7	-26.3	0	2	11.7	13.7	-40
8-12	-26.3	0	0	28.6	28.6	-55
13	-26.3	0	0	69	69	-96
14-15	-26.3	0	0	28.6	28.6	-55
16	-26.3	0	4	9.5	13.5	-40

Table ES. 3 100-Year Design Scour Conditions for Alternative 2

Bent	Initial Bed Elevation (ft-NAVD88)	Degradation (ft)	Contraction Scour (ft)	Local Scour (ft)	Total Scour (ft)	Final Bed Elevation (ft-NAVD88)
2-6	-26.3	0	2	11.7	13.7	-40
7-10	-26.3	0	0	28.6	28.6	-55
11	-26.3	0	0	69	69	-96
12-13	-26.3	0	0	28.6	28.6	-55
14	-26.3	0	4	9.5	13.5	-40

Table ES. 4 100-Year Design Scour Conditions for Alternative 3

Bent	Initial Bed Elevation (ft-NAVD88)	Degradation (ft)	Contraction Scour (ft)	Local Scour (ft)	Total Scour (ft)	Final Bed Elevation (ft-NAVD88)
2-5	-26.3	0	2	11.7	13.7	-40
6-14	-26.3	0	0	28.6	28.6	-55
15-20	-26.3	0	4	9.5	13.5	-40

1 Introduction

FDOT District 1 is evaluating the proposed replacement of the Gulf of Mexico Drive (S.R. 789) Bridge over Longboat Pass, located within Manatee County. As part of the PD&E (Project Development and Environment) study, Scalar Consulting Group (Scalar) has contracted INTERA Incorporated (INTERA) to perform a bridge hydraulic analysis for the replacement bridge. Chapter 2 of this report documents data collection, synthesis, and development of hydrology. Chapter 3 describes hydraulic modeling efforts, including model construction and model simulation results. Chapter 4 details the scour analysis. Finally, Chapter 5 includes additional hydraulic design considerations.

2 Data Collection and Synthesis

Construction of a coastal hydraulic model representative of actual conditions requires a detailed knowledge of the connected waterbodies, bathymetry and topography near the project location, vegetation as well as the location of any structures upstream or downstream of the project, and the bridge geometry as well as the alignment and profile of its approaches.

2.1 Location Map

The proposed bridge will replace the existing S.R. 789 Bridge over Longboat Pass (Bridge Number 130057). The existing bridge was constructed in 1953 and consists of 42 interior bents for a total bridge length of 2,128 ft. Figure 2.1 displays the project location. Longboat Pass is an inlet that conveys flow between the Gulf of Mexico, Anna Maria Sound and Sarasota Bay. FEMA classifies the bridge location as an VE flood zone with a 100-year base flood elevation of +13 ft-NAVD88 according to the 2014 FIRM containing the bridge (Panel 12081C0287E, shown in Figure 2.2).

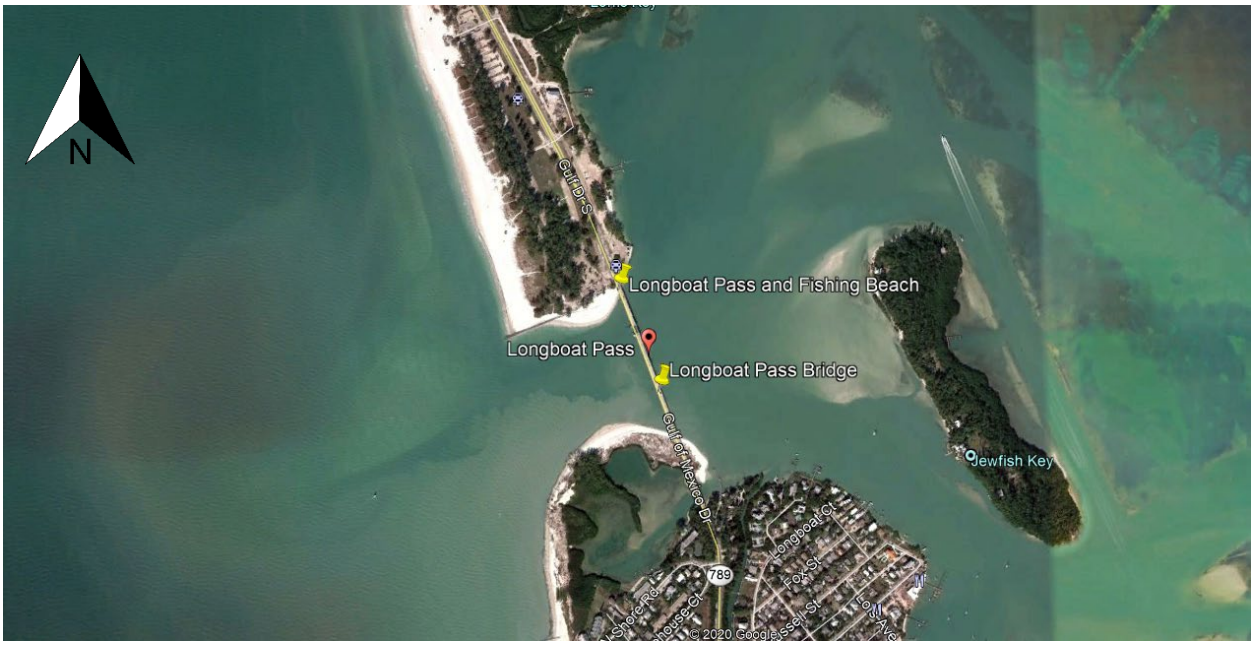

Figure 2.1 Project Location Map

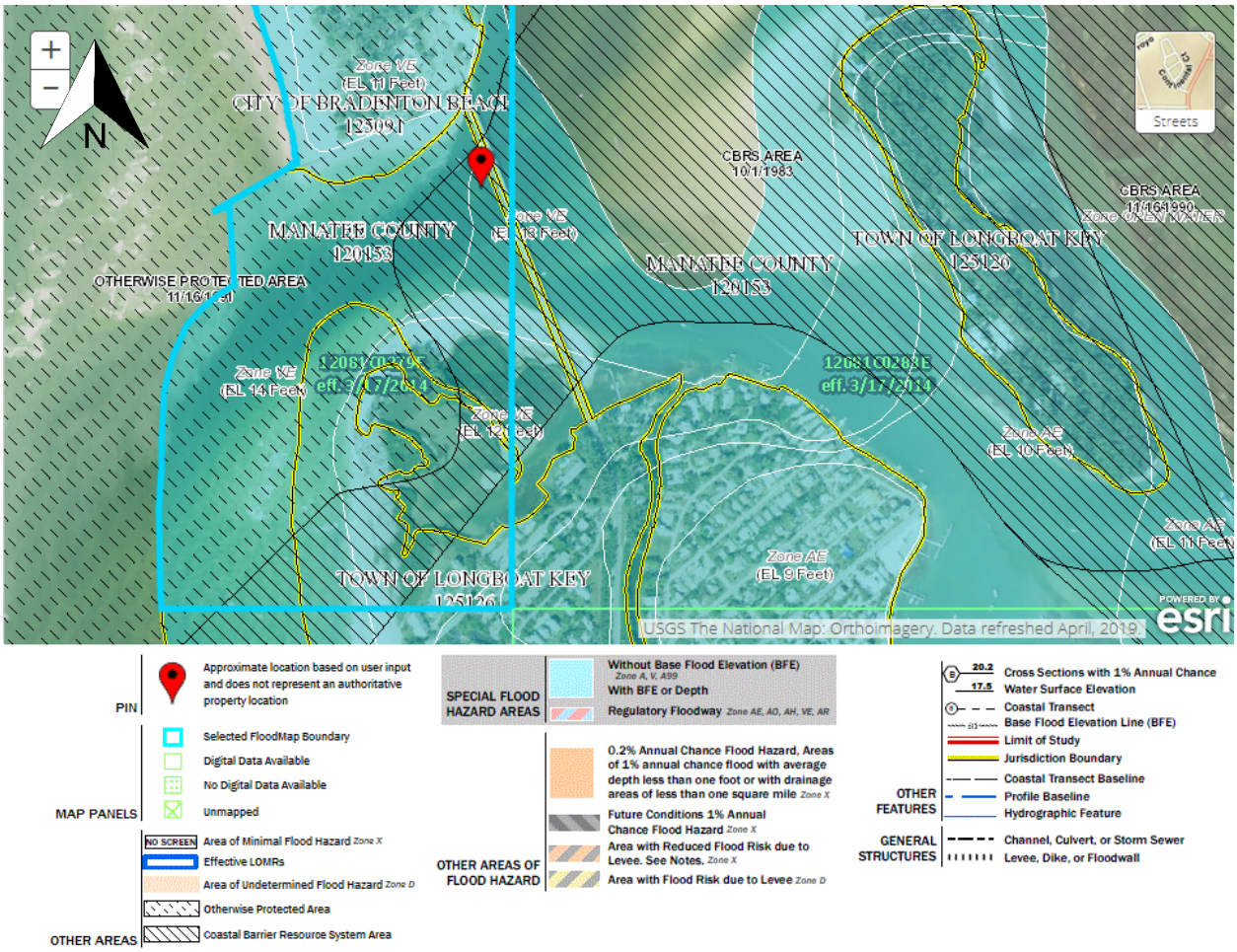

Figure 2.2 2014 FEMA FIRM Panel Containing Project

2.2 FEMA Data

The FEMA FIRM (Figure 2.2) shows a base flood elevation of +13 ft-NAVD88. This elevation includes wave height. The still water elevations determined by FEMA are shown in Figure 2.3 and Figure 2.4 and are a relevant comparison to the model results described in Section 3.4. Longboat Pass is located between transects L1 and BB3 in Figure 2.3, which is from the FEMA Effective FIS in 2014. At this location, the 50-year still water elevation is between +7.3 and +7.8 ft-NAVD88, the 100-year is between +8.9 and +9.3 ft-NAVD88, and the 500-year is between +12.0 and +12.3 ft-NAVD88. From the revised FIS in 2021 (Figure 2.4), Longboat Pass is located between transects 152 and 153. The figure lists the 50-year still water elevation as between +7.3 and +7.4 ft-NAVD88, the 100-year elevation as between +8.4 and +8.8 ft-NAVD88, and the 500-year elevation as between +11.4 and +12.0 ft-NAVD88.

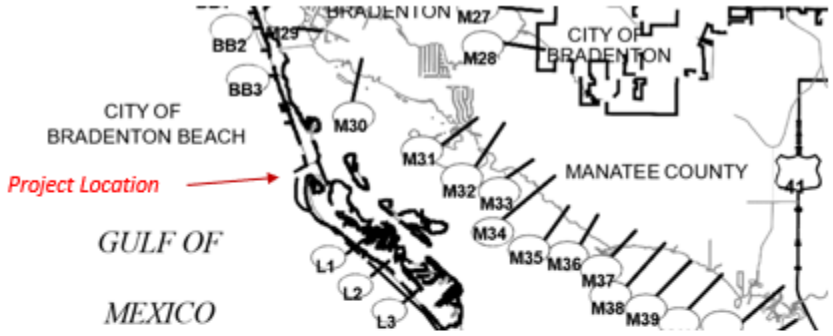

TABLE 8: Summary of Stillwater Elevations

Flooding Source and Location	Stillwater Flood Elevation (Feet NAVD) 10-Year	50-Year	100-Year	500-Year
Gulf of Mexico – City of Bradenton Beach				
Intersection of 26th St. N. and Avenue C	3.4	6.7	8.1	10.9
Intersection of 17th St. N. and Gulf Dr. N.	3.5	7.0	8.6	11.6
Intersection of 13 Street S. and Gulf Dr. S.	3.4	7.3	8.9	12.0
Gulf of Mexico – Town of Longboat Key				
At Lyons Lane	3.7	7.8	9.3	12.3
Sarasota Bay at Bishops Point	4.4	8.3	9.9	12.8

Figure 2.3 Effective FEMA (2014) Stillwater Elevations at Project Location

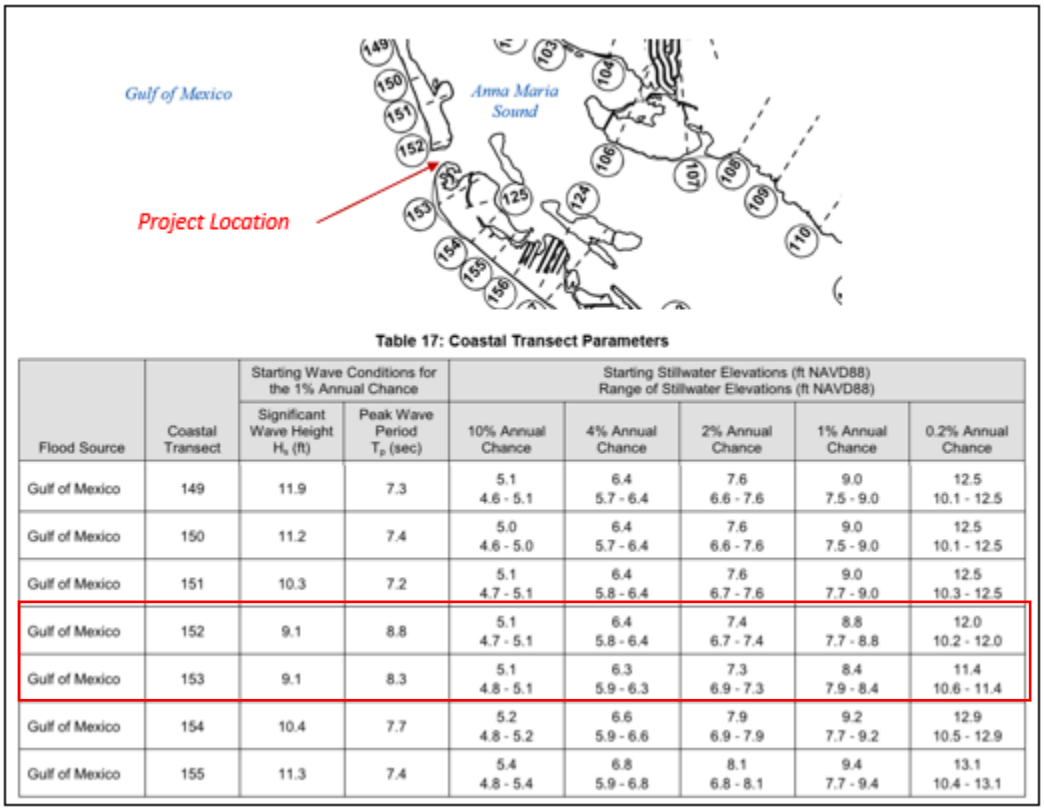

Table 17: Coastal Transect Parameters

Flood Source	Coastal Transect	Starting Wave Conditions for the 1% Annual Chance		Starting Stillwater Elevations (ft NAVD88) Range of Stillwater Elevations (ft NAVD88)				
		Significant Wave Height H_s (ft)	Peak Wave Period T_p (sec)	10% Annual Chance	4% Annual Chance	2% Annual Chance	1% Annual Chance	0.2% Annual Chance
Gulf of Mexico	149	11.9	7.3	5.1 4.6 - 5.1	6.4 5.7 - 6.4	7.6 6.6 - 7.6	9.0 7.5 - 9.0	12.5 10.1 - 12.5
Gulf of Mexico	150	11.2	7.4	5.0 4.6 - 5.0	6.4 5.7 - 6.4	7.6 6.6 - 7.6	9.0 7.5 - 9.0	12.5 10.1 - 12.5
Gulf of Mexico	151	10.3	7.2	5.1 4.7 - 5.1	6.4 5.8 - 6.4	7.6 6.7 - 7.6	9.0 7.7 - 9.0	12.5 10.3 - 12.5
Gulf of Mexico	152	9.1	8.8	5.1 4.7 - 5.1	6.4 5.8 - 6.4	7.4 6.7 - 7.4	8.8 7.7 - 8.8	12.0 10.2 - 12.0
Gulf of Mexico	153	9.1	8.3	5.1 4.8 - 5.1	6.3 5.9 - 6.3	7.3 6.9 - 7.3	8.4 7.9 - 8.4	11.4 10.6 - 11.4
Gulf of Mexico	154	10.4	7.7	5.2 4.8 - 5.2	6.6 5.9 - 6.6	7.9 6.9 - 7.9	9.2 7.7 - 9.2	12.9 10.5 - 12.9
Gulf of Mexico	155	11.3	7.4	5.4 4.8 - 5.4	6.8 5.9 - 6.8	8.1 6.8 - 8.1	9.4 7.7 - 9.4	13.1 10.4 - 13.1

Figure 2.4 Effective FEMA (2021) Coastal Transect Output

Table 2.1 Summary of FIS Still Water Elevations

FEMA Study	50-Year (ft-NAVD)	100-Year (ft-NAVD)	500-Year (ft-NAVD)
Effective Study (FEMA, 2014)	+7.8	+9.3	+12.3
Effective Study (FEMA, 2021)	+7.4	+8.8	+12.0

2.3 Tidal Benchmarks

Figure 2.5 shows the location of the closest open coast NOAA tidal benchmark: 8726243, Anna Maria Outside, FL. Table 2.1 presents tidal datums at this station from the 1983 – 2001 tidal epoch.

Table 2.1 Tidal Benchmark Information at Anna Maria Outside

Tidal Datum Type	Symbol	8726243 Anna Maria Outside Elevation (ft-NAVD88)
Mean Higher High Water	MHHW	+0.64
Mean High Water	MHW	+0.34
North American Vertical Datum	NAVD	0.00
Mean Sea Level	MSL	-0.43
Mean Tide Level	MTL	-0.45
Mean Low Water	MLW	-1.24
Mean Lower Low Water	MLLW	-1.62

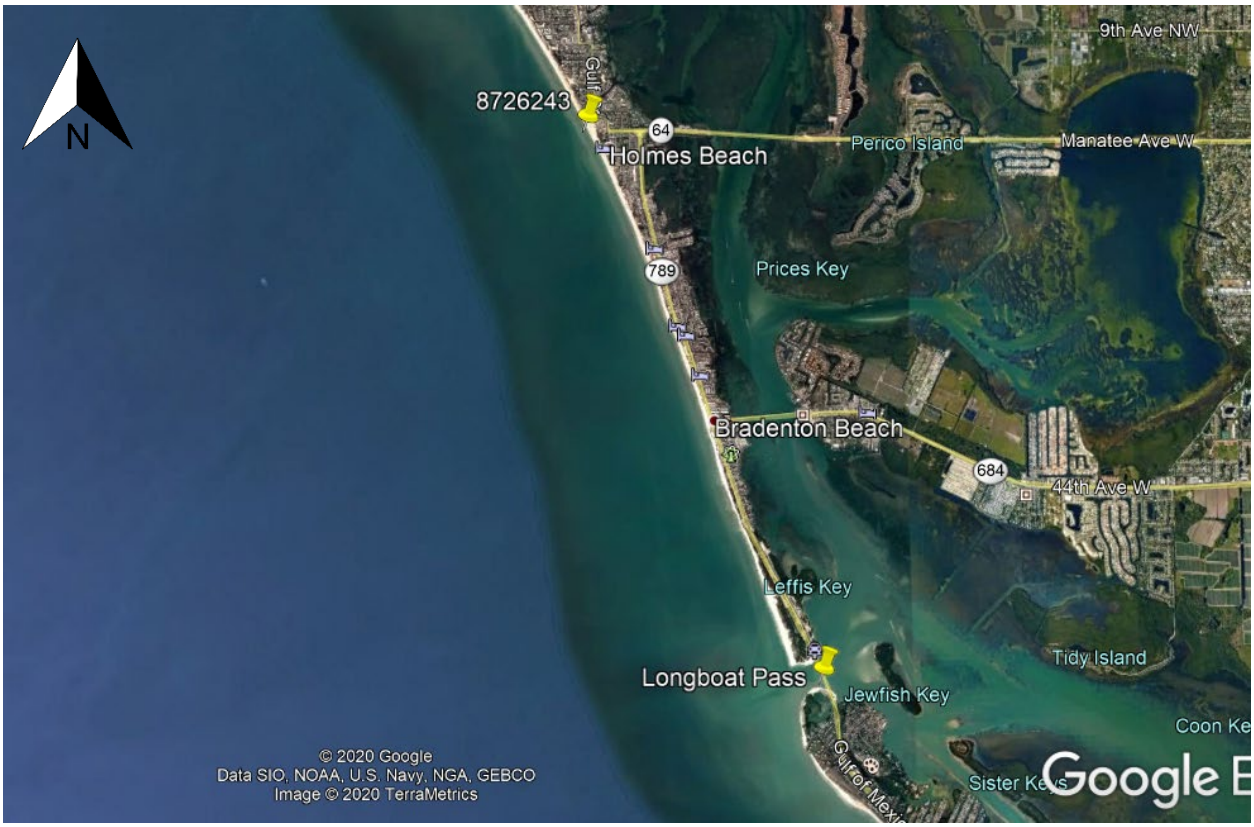

Figure 2.5 Tidal Benchmark Location

2.4 Sea Level Rise Analysis

FDOT Drainage Manual (2023) Section 3.4.1 requires sea level rise to be included in new designs and describes a methodology based on historical analysis of long-term NOAA tidal stations. The nearest tidal station for analyzing sea-level rise is the NOAA station at Clearwater Beach, FL (Station ID: 8726724). FDOT requires using the straight-line regression extrapolation for this gage to develop sea-level rise. At

Station 8726724, this rate is 4.22 mm/yr. MSL for NOAA tidal benchmarks is reported for the 1983-2001 tidal epoch. Sea-level rise was calculated from the midpoint of this period (1992) and projected to the end of service date for the new bridge (assuming 75-year design life and construction completion in 2022). This results in a sea-level rise of 1.45 ft.

2.5 Elevation Data

Construction of the two-dimensional ADCIRC model mesh (Chapter 3) requires knowledge of bathymetry and topography near the project. For this project, USACE's Longboat Pass channel survey data was supplemented with 2006 Manatee County LiDAR data and the 2013 USGS 1/9th degree Digital Elevation Model (DEM). Figure 2.6 shows the elevation contours near the bridge.

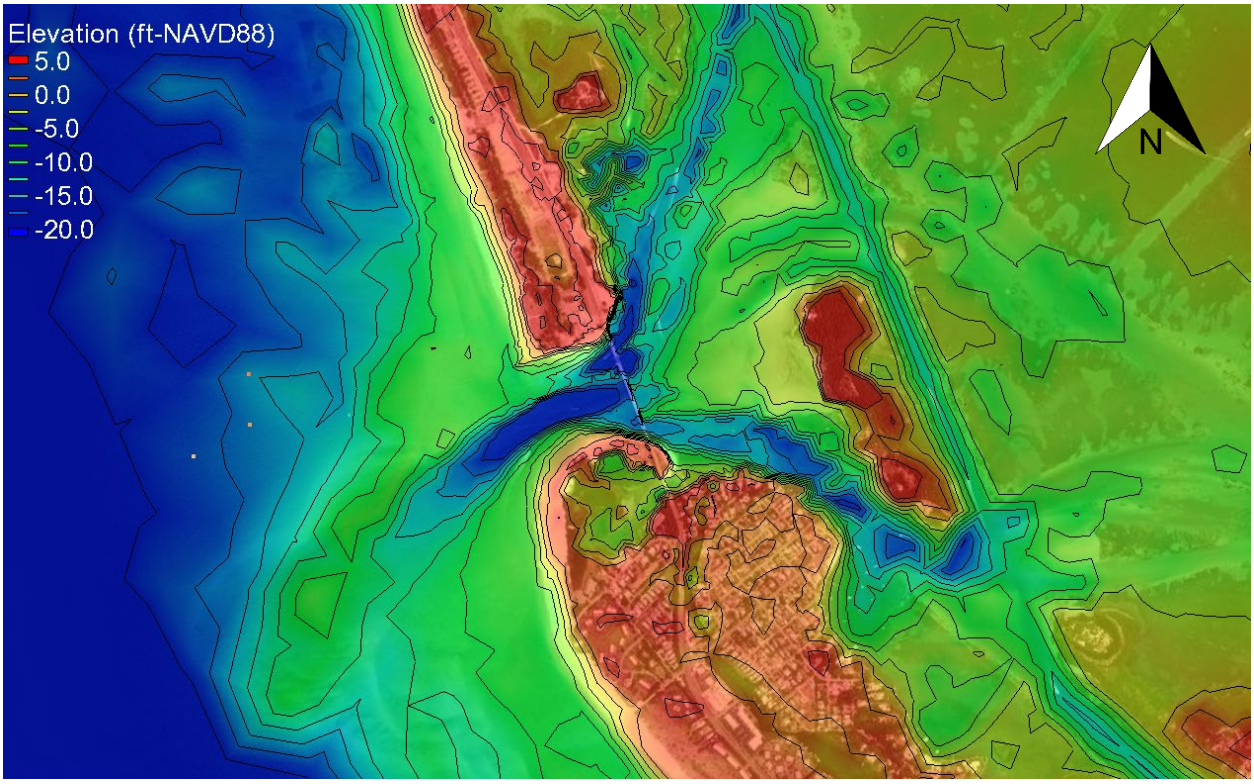

Figure 2.6 Elevation Contours Near the Bridge

2.6 Geotechnical Information

The local scour and contraction scour calculations described in Chapter 4 of this report require the sediment median diameter (D50) as input. As no D50 was provided for this PD&E study, a standard value of 0.2 mm was applied to the scour analysis contained in Chapter 4.

2.7 Wind Field

The hydrodynamic modeling effort described in Chapter 3 is forced by hurricane wind and pressure fields to drive storm surge and wave conditions. The wind field is applied at the water surface as shear stresses simulating the passage of a hurricane over the project location. Wind fields are preferred over offshore storm surge hydrographs because the model then captures the effects of local wind setup at the bridge. For this project, the wind and pressure field hindcast of the 1921 Tarpon Springs hurricane were modified to drive the SWAN+ADCIRC simulations. Storm surge is a function of wind speed, storm path, storm forward

speed, atmospheric pressure, storm horizontal extents and energy, and bathymetry. For this project, the wind field intensity was iteratively scaled until storm surge elevation produced at the open coast matches the predicted still water range provided for the nearest coastal transect contained in the 2021 FEMA Manatee County Flood Insurance Study (FIS) (Transect 152, see Section 2.2). Table 2.2 lists the values provided by FEMA at transect 152, the ADCIRC model results, and the iteratively determined multiplication factor to produce storm surge matching the FEMA values.

Table 2.2 Determined Wind Scaling Factor

Return Period	2021 FEMA FIS Elevation (ft-NAVD88)	ADCIRC Model Elevation (ft-NAVD88)	Wind Field Scaling Factor
50-year (2%)	+7.4	+7.6	1.19
100-year (1%)	+8.8	+8.9	1.25
500-year (0.2%)	+12.0	+11.8	1.41

2.8 Structure Geometry

Three alternatives have been designed for the replacement bridge. Alternative 1 is a bascule bridge, 2,160'-5" long with a span arrangement of 5@91'-9"-7@152'-8"-175'-3@152'8". The proposed replacement structure will have an out-to-out width of 76'-8". The proposed bridge substructure consists of complex piers except for bascule pier 13. The columns are 6' x 10'. The pile caps are 26' x 26' x 7' with a 3' thick seal to accommodate 16 (4x4) 24" square reinforced concrete piles spaced 6' on center. The pile cap elevation is at +4 ft-NAVD88. The bascule pier is 57' x 96' with a pile cap of 59' x 98' x 7' (with a 3' thick seal). The low member elevation within the main span is at +26.06 ft-NAVD88. The low member elevation for the entire bridge is at +14.6 ft-NAVD88. Figure 2.7 displays the details of the complex pier provided by Scalar.

Alternative 2 is also a bascule bridge, 2152' long with a span arrangement of 2@72'-6"-9@152'-8"-175'-3@152'8". The proposed replacement structure will have an out-to-out width of 76'-8". The proposed bridge substructure consists of the same type of complex piers and bascule pier as alternative 1 except that the bascule pier is located at pier 11. The low member elevation within the main span is at +39.06 ft-NAVD88. The low member elevation for the entire bridge is at +16.10 ft-NAVD88.

Alternative 3 is a fixed bridge, 3,100' long with a span arrangement of 20@155'. The out-to-out width is also 76'-8". The proposed bridge substructure consists of the same type of complex piers as alternative 1 and 2. The low member elevation within the main span is at +81.06 ft-NAVD88. The low member elevation for the entire bridge is at +19.00 ft-NAVD88.

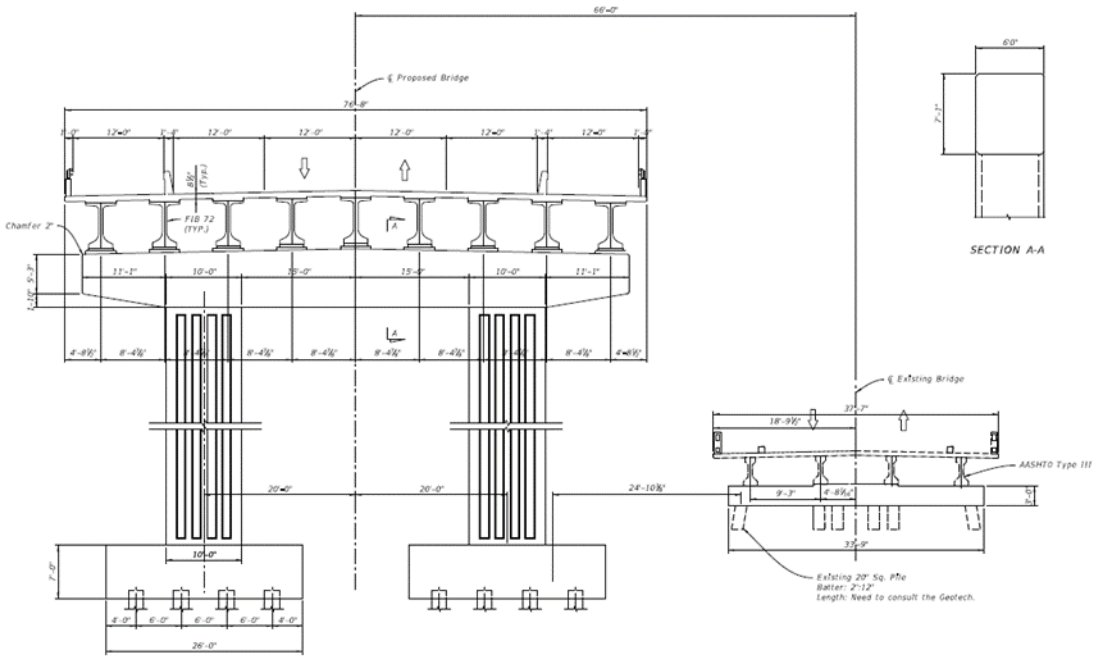

Figure 2.7 Details of the Complex Pier (Source: Scalar)

2.9 Field Review

On February 26, 2020, INTERA personnel visited the project site. The site visit provides a basis for specification of model friction values near the bridge. Additionally, the visit provides an opportunity to observe characteristics that may not be apparent from project surveys, aerial imagery, inspection reports of the existing structure, or plans of the existing structure.

The channel was free of vegetation and obstructions on both sides of the bridge (Figure 2.8 and Figure 2.9). The inlet is highly dynamic over time, presently a bulkhead near the north bridge end limits migration to the north. A jetty-like structure filled with riprap between piles resides west of the north bridge end and reduces littoral transport of sand into the pass. An adjacent geotube further restricts longshore sediment transport. There are no bulkheads or other shoreline stabilization features near the south bridge end, however the shoreline is less exposed and therefore less dynamic than at the north bridge end. That said, the land separating Longboat Pass and the lagoon has evolved significantly over time. Further discussion of historic inlet evolution and shoreline migration is presented in Section 4.1.2. Appendix D includes more field visit photos.

Figure 2.8 East Bridge Face

Figure 2.9 West Bridge Face

3 Hydraulic Modeling

Scour computations require flow information, including flow velocity, depth, and direction. Determining these parameters requires a detailed hydraulic analysis of the study area. The complexity of flow conditions at the bridge site dictated the method employed in this analysis. These conditions result from hurricane surge propagating through Longboat Pass to Anna Maria Sound and Sarasota Bay from the Gulf of Mexico.

Given the project's location and connectivity to the Gulf of Mexico, a hydrodynamic model capable of simulating hurricane storm surge is necessary for this project. The ADCIRC model is well suited to the task and has been used for storm surge hydraulic analyses for many bridges throughout Florida and the southeastern US, and it was therefore selected for application on this project.

3.1 Model Setup

ADCIRC, a numerical model developed specifically for generating long duration hydrodynamic circulation along shelves, coasts, and within estuaries, produces numerical simulations for very large computational domains in a unified and systematic manner. ADCIRC employs computational models of flow and transport in continental margin waters to predict free surface elevation and currents for a wide range of applications including evaluating coastal inundation, defining navigable depths and currents in near shore regions, and assessing pollutant and/or sediment movement on the continental shelf.

ADCIRC solves the equations of motion for a moving fluid on a rotating earth. The equation formulation includes applying the traditional hydrostatic pressure and Boussinesq approximations and discretizing the equations in space via the finite element method and in time via the finite difference method. The ADCIRC program includes both a two-dimensional depth integrated (2DDI) mode and a three-dimensional (3D) mode. For both, the model solves for elevation via the depth-integrated continuity equation in Generalized Wave-Continuity Equation form. The model solves for velocity via either the 2DDI or 3D momentum equations. These equations retain all of the nonlinear terms.

The program simulated both the tidal circulation and the hurricane storm surges in the project area. Possible boundary conditions for the model include

- specified elevation (harmonic tidal constituents or time series);
- specified boundary normal flow (harmonic tidal constituents or time series);
- zero boundary normal flow;
- slip or no slip conditions for velocity;
- external barrier overflow out of the domain;
- internal barrier overflow between sections of the domain;
- surface stress (wind and/or wave radiation stress);
- atmospheric pressure; and
- outward radiation of waves (Sommerfield condition)

For this application, the inputs to the ADCIRC model include a bathymetric/topographic unstructured mesh, hindcasted wind and pressure fields, tidal potentials, and wave radiation stresses from SWAN.

In addition to providing wave radiation stresses, SWAN simulated wave heights and periods. The wave action balance equation with sources and sinks (Holthuijsen et al., 2003) forms the basis of the model. Wave propagation processes represented include propagation through geographic space, refraction due to spatial variations in bottom and current, shoaling due to spatial variations in bottom and current, blocking and reflections by opposing currents, and transmission through, blockage by, or reflection against obstacles. Wave generation and dissipation processes represented include generation by wind; dissipation by white-capping, depth-induced wave breaking, and bottom friction; and wave-wave interactions. The model

contains both stationary and non-stationary operational modes formulated for Cartesian, curvilinear, or spherical coordinate systems.

The inputs to the SWAN model include a bathymetric/topographic unstructured mesh, hindcasted wind field, water surface elevation, and currents from ADCIRC.

3.2 Model Development

Figure 3.1 shows the mesh extent and mesh geometry at Longboat Pass. The mesh contains bathymetry interpolated from NOAA datasets for both nearshore (coastal relief data set) and open ocean (ETOPO2, ETOPO5) regions, 2007 county LiDAR data, USGS 1/9th degree topographic DEM data, and USACE's Longboat Pass channel survey data. This study provided increased mesh resolution near the project location to accurately depict pertinent topographic and bathymetric features affecting flow regime.

The mesh covers the western North Atlantic Ocean, the Gulf of Mexico, and the Caribbean Sea. The mesh includes more than 136,000 triangular elements with over 70,000 nodes located at the corners of the elements. Multiple sources provided the data to refine the constructed mesh.

This study modified the calibrated model mesh developed for a previous modelling study within Tampa Bay. Specifically, this study refined a portion of that model mesh lying along the Gulf of Mexico, Anna Maria Sound, and Sarasota Bay including Longboat Pass. Extra detail was added to the project site and S.R. 789 roadway approaches and the bridge. Figure 3.1 displays the ADCIRC model mesh and Figure 3.2 shows mesh elevation contours globally and near the project location.

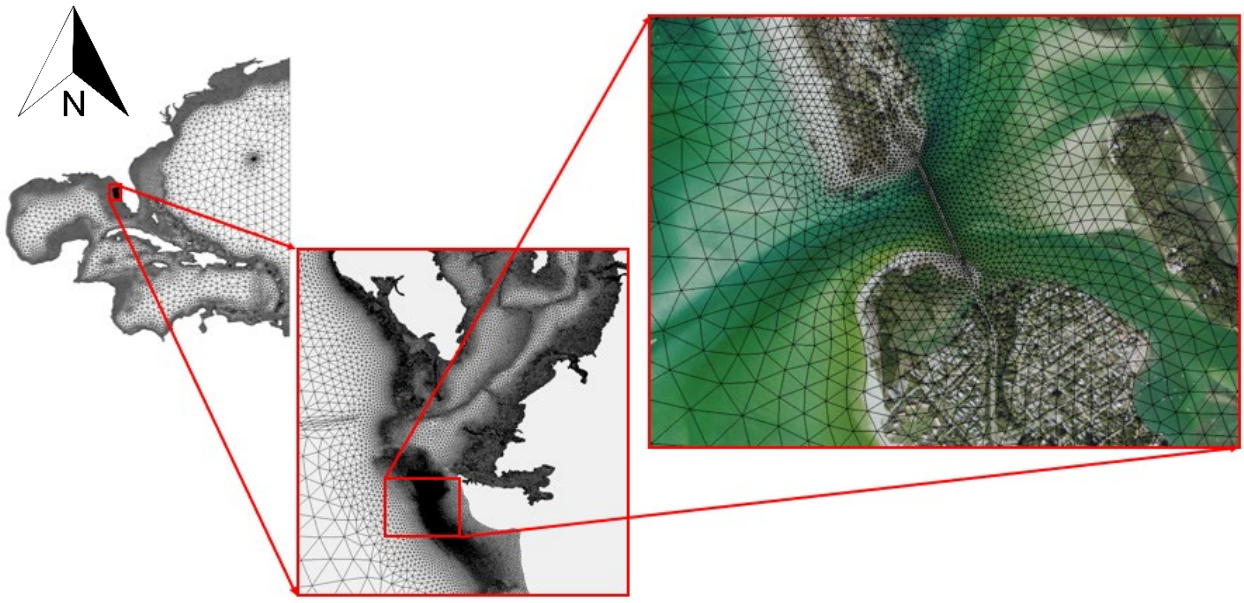

Figure 3.1 ADCIRC Model Mesh Extent and View of Mesh at Project Location

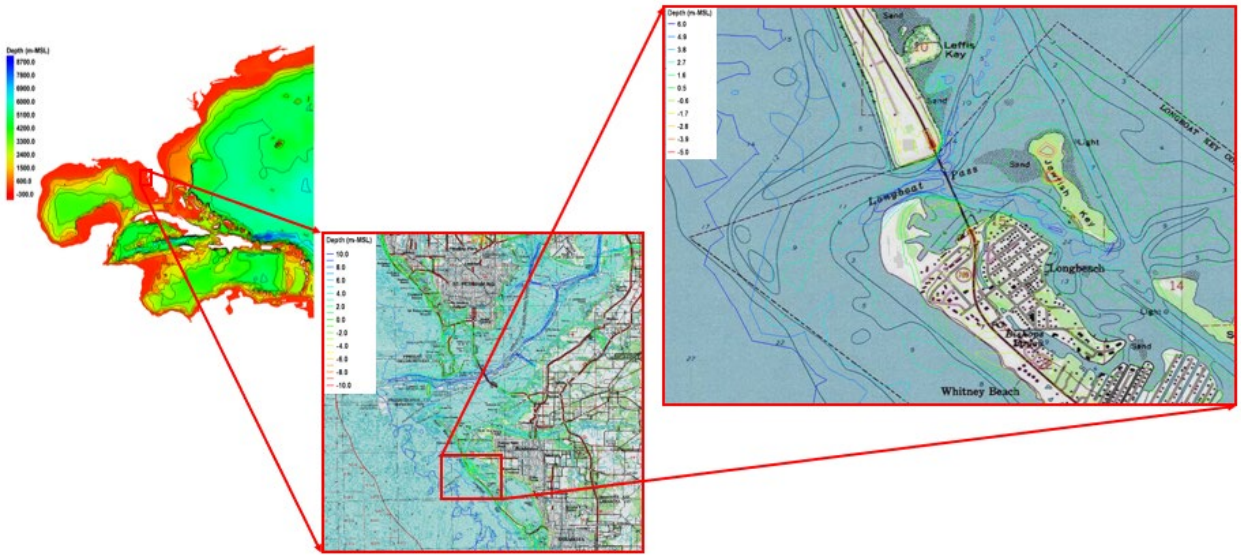

Figure 3.2 ADCIRC Model Mesh Elevation Contours

3.3 Model Calibration

Model calibration involves an iterative process of adjusting model parameters until the model results at a set location closely match measured data at that location. Model calibration was completed for the coastal Gulf of Mexico through comparison with measured tidal data at NOAA's Clearwater Beach tide station and within Tampa Bay at the NOAA Port Manatee Tide station. This calibration ensures that model friction and other control parameters are set reasonably for surge propagation in the nearshore Gulf of Mexico.

Model calibration applies the following error estimations as a quantitative method to judge their ability to reproduce measured events. The first equation provides an estimate of the mean error (E), the average of the deviation of the calculated from the measured values defined as

$$E = \frac{\sum_{i=1}^{N} (\chi_c - \chi_m)_i}{N} \tag{3.1}$$

where χ_c is the calculated value, χ_m is the measured value, and N is the total number of data points. A positive value for the mean error would indicate that the model overestimates the event, while a negative value would indicate the model underestimates the event.

The root-mean square error (E_{rms}) indicates the absolute error of the comparison. Equation 3.2 defines this error as

$$E_{rms} = \sqrt{\frac{\sum_{i=1}^{N} (\chi_c - \chi_m)_i^2}{N}} \tag{3.2}$$

Calibration involved the adjustment of model friction and lateral eddy viscosity until modeled water surface elevations and wave heights matched measured values fall within acceptable error range. FEMA (2007)

defines this range as 10% or less for tidal calibrations. For storm surge verifications, FEMA acknowledges the complexity associated with measurements during storms. Based on that complexity, FEMA notes that the acceptable error range will exceed values expected under normal tidal calibrations. Calibration of the model involved simulation of water surface elevation fluctuations for tides from June 28, 2005 to July 7, 2005.

Figure 3.3 and Figure 3.4 compares the measured water surface elevations with the hindcasted simulation in Clearwater Beach (NOAA Station 8726724) and Port Manatee (NOAA Station 8726384), respectively. In the figures, the orange line represents the ADCIRC simulated water surface elevation and the blue line represents the measured values. As the figure demonstrates, the simulated water surface and the measured values agree during the tide. Table 3.1 summarizes the results of the calibration. In the table, mean error is the average of the deviation of the calculated from the measured values, the root-mean square error (RMS) is a measure of the absolute value of the error, and the percent error gives an indication of the degree to which the modeled values represent the measured values. As the table shows, the errors at each gage are within FEMA's acceptable error range; as such, the model calibration is considered verified.

Table 3.1 Summary of the ADCIRC+SWAN Storm Surge Calibration.

Gage	Mean Error (ft)	RMS (ft)	Percent Error
NOAA Gage 8726724	0.029	0.059	4.9%
NOAA Gage 8726384	0.038	0.058	5.9%

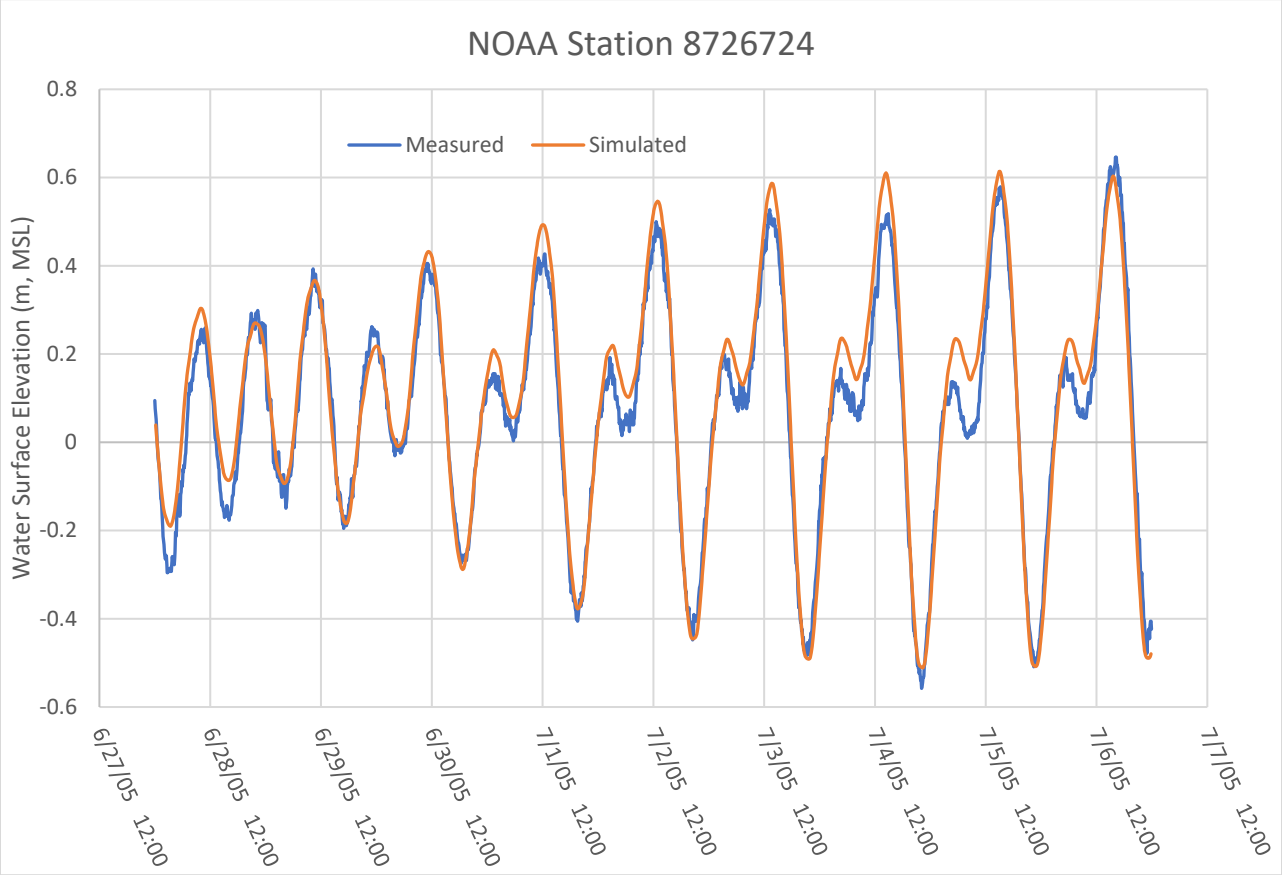

Figure 3.3 Comparisons of Measured and Modeled Water Surface Elevations for Clearwater Beach

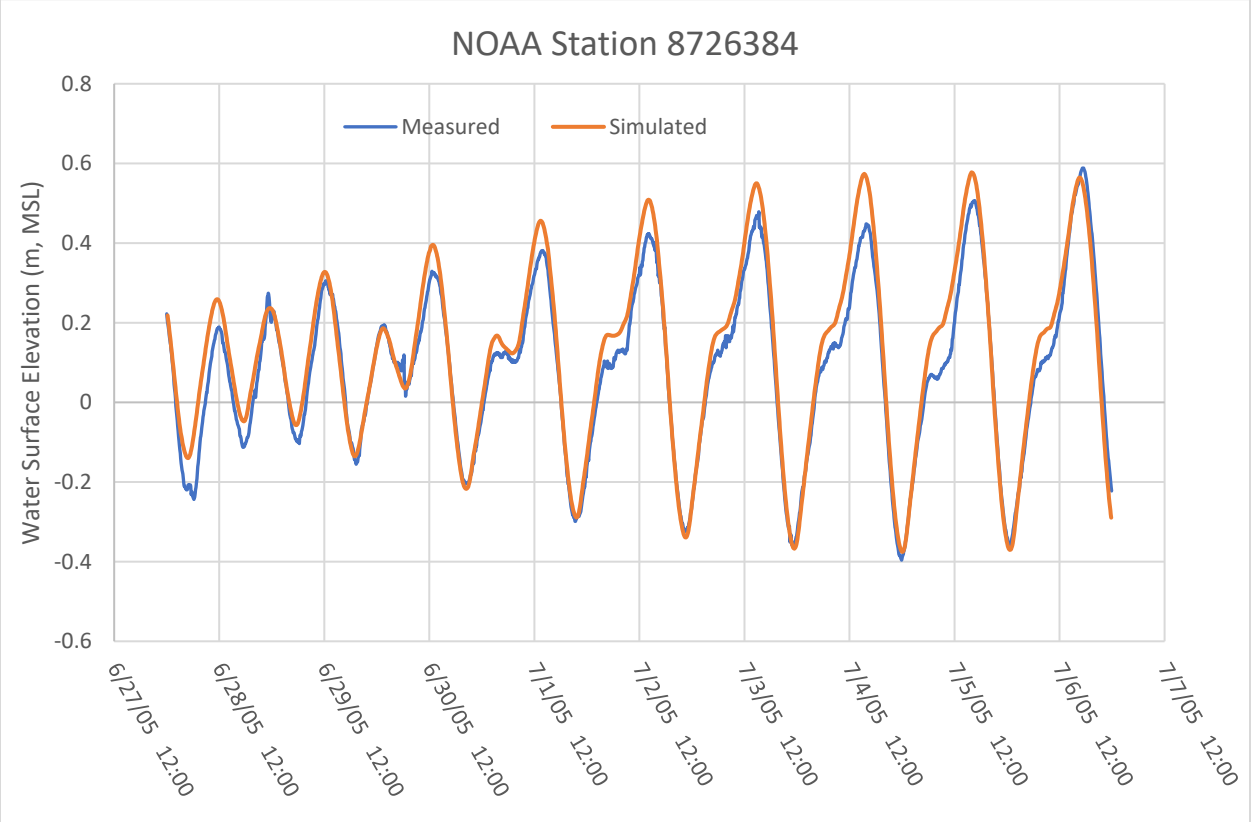

Figure 3.4 Comparisons of Measured and Modeled Water Surface Elevations for Port Manatee

3.4 Model Results

Local scour and contraction scour depths are very sensitive to input flow conditions. Providing reasonable flow velocity and depth inputs is critical for accurate scour depth predictions. Modeling efforts described in this chapter form the basis of flow inputs for the scour calculations detailed in Chapter 4. The water surface elevation, velocity magnitude, and discharge time series plots at the bridge for the 50-, 100-, and 500-year event are shown in Figure 3.5 through Figure 3.7. The 500-year water surface elevation and velocity magnitude are greater than those of the 100-year ones which are greater than the 50-year ones. Contour plots of water surface elevation and flow velocity magnitude for the 50-, 100-, and 500-year events near the bridge are presented in Figure 3.8 through Figure 3.10. The flow approaches the bridge opening almost perpendicularly. Table 3.2 summarizes results for the 50-, 100-, and 500-yr scenarios at the model cross section upstream of the bridge. Notably, the modeling predicts a greater flow through the channel during the 100-year event as compared with the 500-year event. This is attributed to the significant overtopping that occurs during the 500-year storm surge. Additionally, the stage elevation including a SLR of 1.45 ft (Section 2.4) was also presented in Table 3.2.

Table 3.2 Summary of Model Results at Bridge for Simulations

	Design (50-Year) Flood	Base (100-Year) Flood	Greatest (500-Year) Flood
Stage Elevation w/o SLR (ft-NAVD88)	+7.6	+8.9	+11.8
Stage Elevation w/ SLR (ft-NAVD88)	+9.1	+10.3	+13.3
Discharge w/o SLR (cfs)	218,319	227,383	220,318
Velocity w/o SLR (ft/s)	10.8	10.9	11.4
Exceedance Probability (%)	2	1	0.2
Frequency (yr)	50	100	500

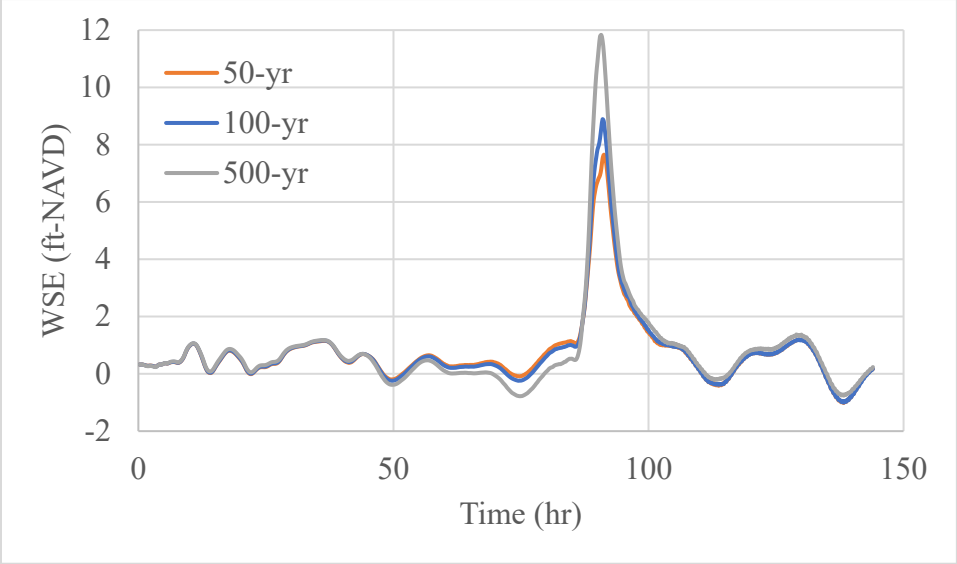

Figure 3.5 Water Surface Elevation Time Series at Bridge (without Sea-Level Rise)

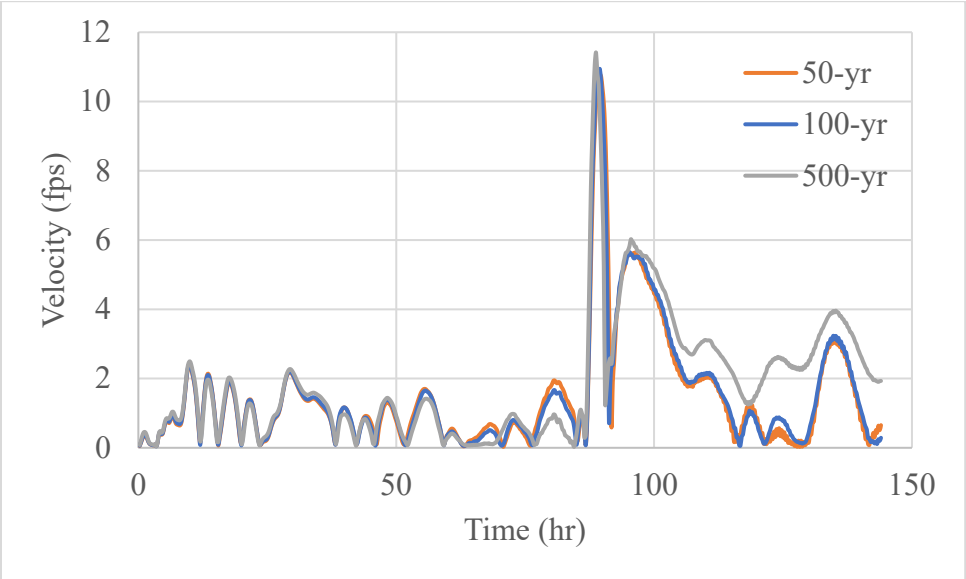

Figure 3.6 Velocity Magnitude Time Series at Bridge (without Sea-Level Rise)

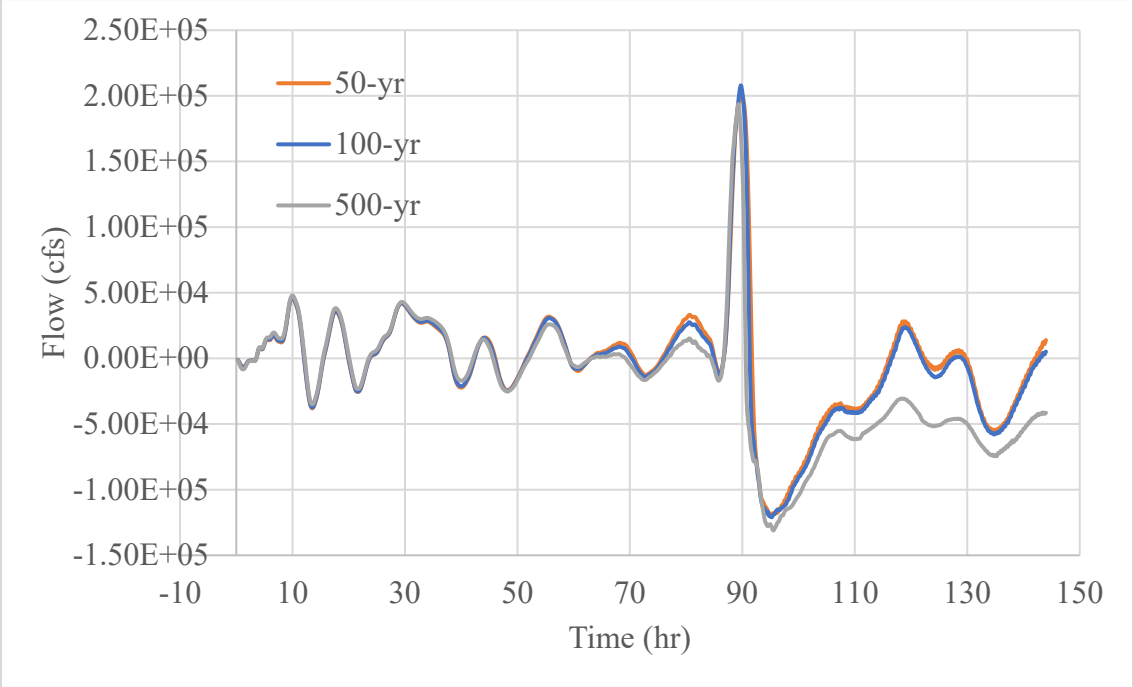

Figure 3.7 Flow Discharge Time Series through Bridge (without Sea-Level Rise)

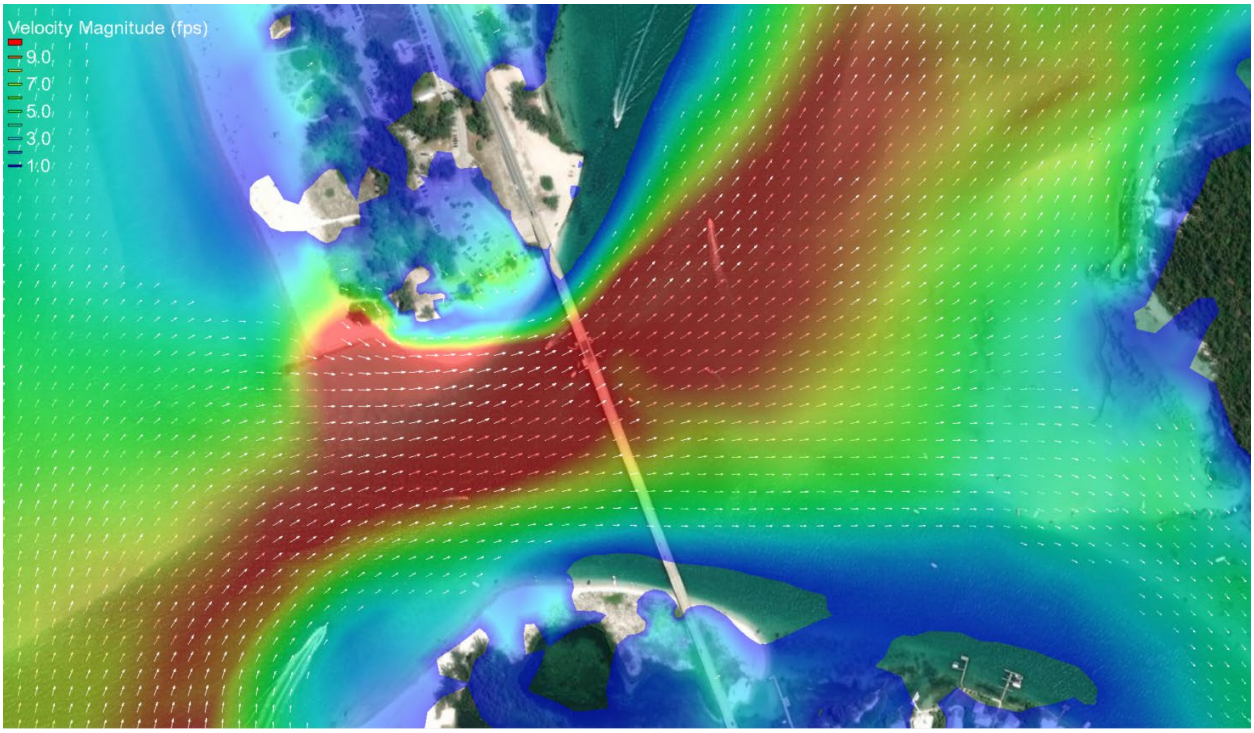

Figure 3.8 50-Year Peak Flow Velocity Magnitude Contours (without Sea-Level Rise)

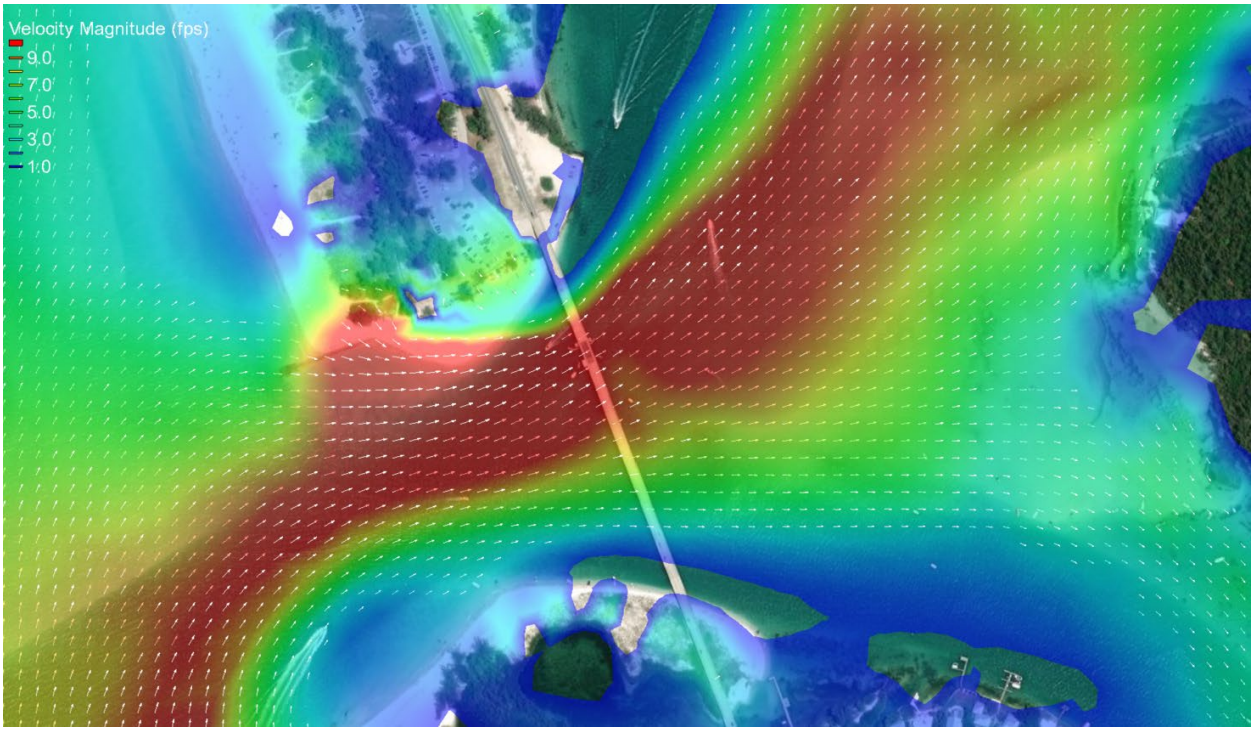

Figure 3.9 100-Year Peak Flow Velocity Magnitude Contours (without Sea-Level Rise)

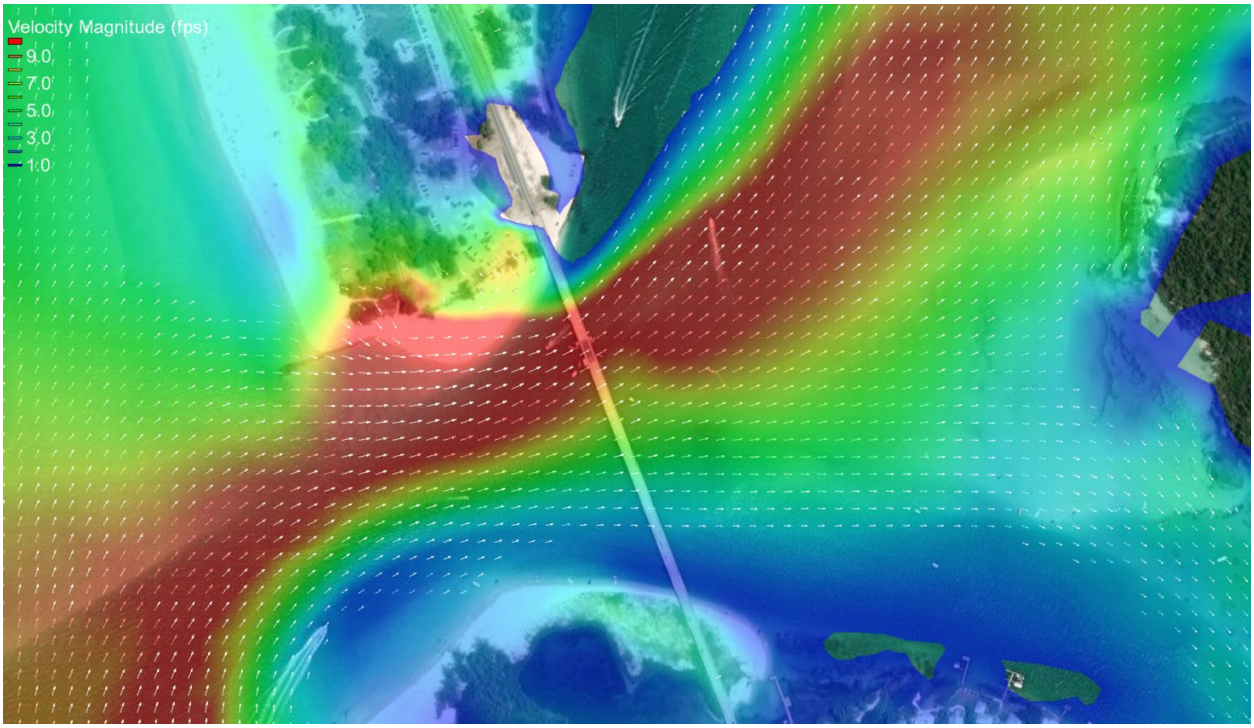

Figure 3.10 500-Year Peak Flow Velocity Magnitude Contours (without Sea-Level Rise)

3.5 Wave Climate

Wave climate is an important design parameter for coastal bridges. The 100-year wave crest elevation is a key element in setting the low chord elevation of the superstructure. If the bridge superstructure is within the wave crest, then the superstructure design must consider wave forces.

Figure 3.11 presents contours of the significant wave — the average height of the one-third highest waves occurring in a sample (typically 30-minute-long sample). As the figure illustrates, the largest waves — up to 4 feet — occur near the center of the channel. Figure 3.12 presents the wave crest elevation at the channel centerline at the bridge throughout the duration of the 100-year simulation without SLR. The wave crest elevation is +15.1 ft-NAVD including SLR (13.6’ + 1.45’).

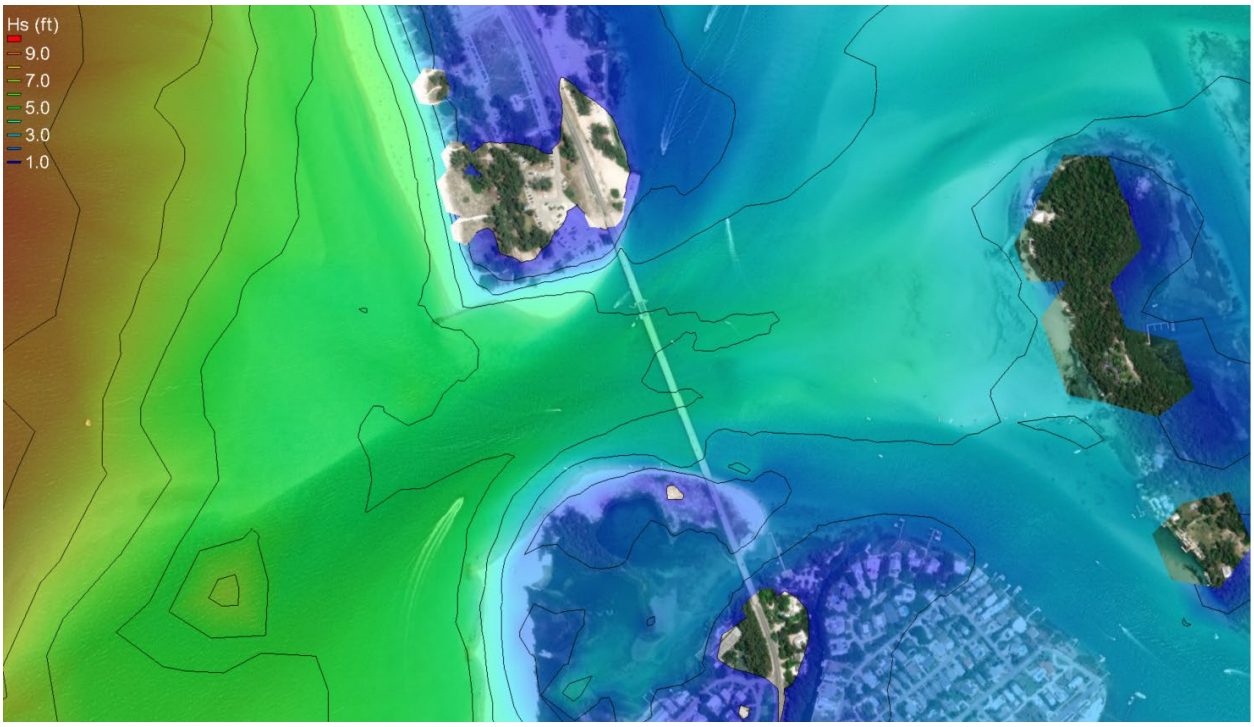

Figure 3.11 100-Year Significant Wave Height

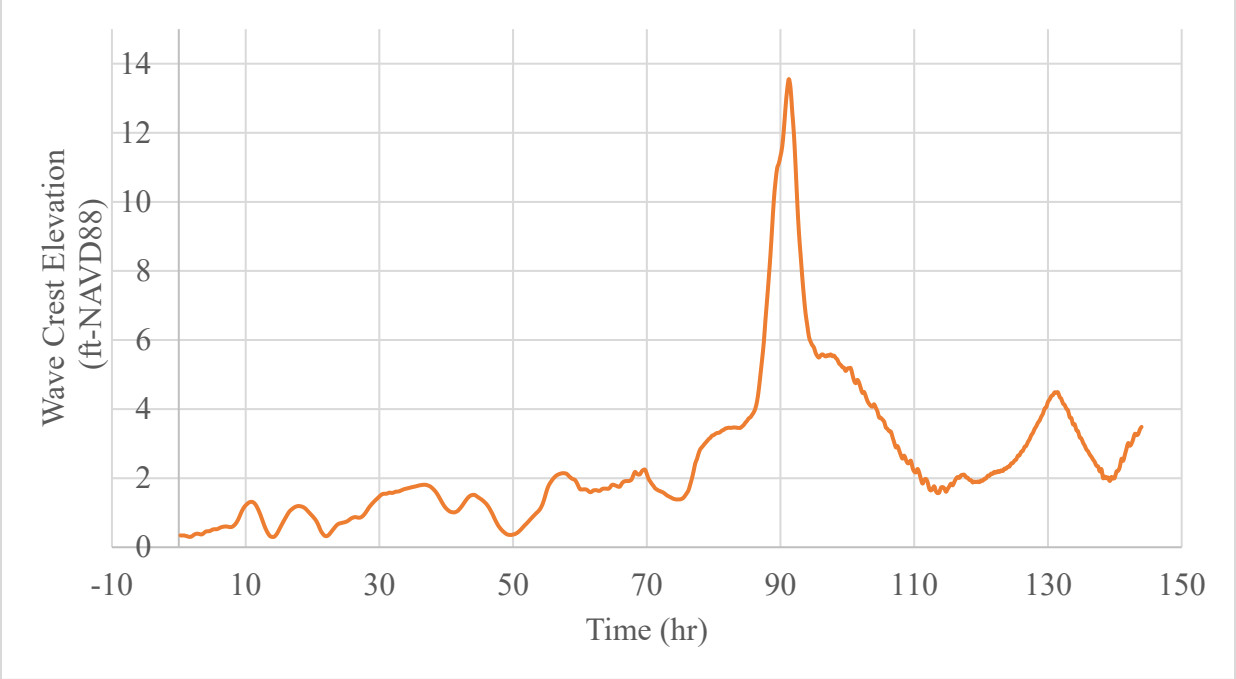

Figure 3.12 100-Year Wave Crest Elevation w/o SLR Time Series Plot

4 Scour Analysis

Total scour consists of three components: (1) long-term scour (aggradation/degradation and channel migration), (2) contraction scour, and (3) local scour. Unlike long-term scour, the contributions of local and contraction scour are derived from the results of the hydraulic analysis presented in Chapter 0. Their corresponding scour computations apply empirical equations developed by FDOT in conjunction with the University of Florida (Sheppard & Renna, 2013). The formulation of the complex pier scour calculation methodology follows techniques described in the Hydraulic Engineering Circular No. 18 (HEC-18) (Federal Highway Administration, 2009). These equations require inputs such as stream flow rate, local velocities (magnitude and direction) at the piers, and depth of flow. The model simulations presented in Chapter 3 provide the values for these parameters. This chapter discusses scour components and the results of these scour calculations for the proposed bridge.

Scour depth computations require values for the depth-averaged critical velocity of the waterway necessary to initiate sediment motion on the bed. Calculating the onset of sediment transport, requires a representative median sediment size (D50 equals 0.2 mm). This study contains scour calculations for the 100-year design event and the 500-year check event for the bridge. Scour associated with these two events was calculated employing the hydraulic model results presented in Chapter 0 as inputs. The following three sections detail long-term scour, contraction scour, and local pier scour.

4.1 Long Term Scour

Most of the bridges in the National Bridge Inventory (NBI) that cross alluvial streams continually adjust their beds and banks (Federal Highway Administration, 2012). Channel stability at the bridge crossing depends on the stream system. Changes upstream and downstream affect stability at the bridge crossing. Natural and man-made disturbances may result in changes in sediment load and flow dynamics resulting in adverse changes in the stream channel at the bridge crossing. These changes may include channel bank migration, aggradation, or degradation of the channel bed. During channel migration, one bank tends to erode laterally while the opposite bank tends to accrete. During aggradation or degradation of a channel, the channel bed and thalweg tend to accrete or erode.

Channel stability, as characterized by channel migration and aggradation/degradation of the channel bed, is an important consideration in evaluating the potential scour at a bridge for two reasons. First, because aggradation and degradation influence the channel's hydraulic properties, any hydraulic modeling must consider their effects when determining design scour conditions. Second, bank migration, thalweg shifting, and degradation may cause foundation undermining regardless of whether the bridge experiences the design storm event. This section presents an analysis of channel migration and aggradation/degradation of the channel bed at the bridge opening. This analysis forecasts channel stability based on historic observations near the bridge. The analysis incorporates a review of available historic aerials in the vicinity of the bridge. These help to evaluate channel migration and thalweg position within the channel banks and aggradation or degradation of the bed.

4.1.1 Aggradation/Degradation

Aggradation and degradation refer to the long-term raising or lowering of the stream bed. Aggradation and degradation are the result of excess or insufficient sediment transport in a stream to maintain its bed elevation. Aggradation and degradation are typically long-term processes, but significant changes in an upstream drainage basin, such as the installation of a dam or the construction of a large development resulting in a drastic change in land-use, may result in accelerations in aggradation or degradation. The most reliable method for assessing aggradation and degradation is through comparison of historic bed profiles at the bridge crossing. As no bridge inspection reports for the existing bridge were provided, no

historic bed profiles can be accessed. However, the inlet is influenced by tidal flows and the bridge thalweg is expected to remain relatively stable. Therefore, the bed degradation component of scour is set to zero.

4.1.2 Lateral Migration Analysis

While bridges are static structures, inlets often exhibit dynamic behavior with shifting bank lines via erosion and accretion over time. The historic record of maps, survey, and aerial imagery is used to understand waterway evolution at the project location. For this project, the oldest record is a US Coast and Geodedic Survey chart from 1883 that serves as a predevelopment baseline prior to human modifications. In 1889, the US Army Corps of Engineers (USACE) performed the first improvement feasibility and economic justification study. Figure 4.1 illustrates the 1883 MHW survey overlaid on a current aerial image to show the change in the channel, inlet shape, and shoreline locations.

The inlet underwent significant change between 1883 and 1940 as shown in the 1883 shoreline overlaid on the 1940 aerial in Figure 4.2. The first recorded structure traversing the inlet was the Longboat Pass Bridge constructed in 1927 and destroyed by storm surge in a March 1932 storm.

Due to the dominant nature of the northern inlet channel, the more restrictive south inlet channel closed prior to 1952, changing the dynamics and resulting in the formation of a sand spit on the north end of Longboat Key; also, by 1955, prior surveys were compared and determined that significant erosion had occurred along the south end of Anna Maria Key, prompting the construction of the current jetty structure in 1957. By 1962, the south end of Anna Maria Key had recovered significantly after the jetty construction, while the sand spit on the north end of Longboat Key breached (Figure 4.3). In 1958, the Longboat Pass Bridge was completed; it is a bascule type bridge that remains in service today.

It wasn't until 1969 that the sand spit reformed on the north end of Longboat Key after equilibrium was reached at the south end of Anna Maria Key. From that point until 1973, the north end of Longboat Key experienced significant accretion on the Gulf side while the inlet channel remained virtually unchanged (Figure 4.4).

After 1973, the main changes occurred on the sand spit found on the north end of Longboat Key, land feature initially recognized in 1952 aerial photography. From the time of its formation until 1973, a significant amount of vegetation had grown on the north end of the hook-shaped sand spit. From 1973 to 1977 the tip of the "hook" had expanded eastward and thickened its connection to Longboat Key as well as the development of housing (a) immediately south of the sand spit had occurred; by 1980, the tip expanded further east and the Gulf side beach of Longboat Key had expanded westward. On the south side of Anna Maria Key, the seawall demonstrated to start leaking sand into the channel from its eastern end towards the west, and by 1980 the width of the inlet had reduced significantly. Figure 4.5 shows the 1977 Survey shoreline overlaid onto the aerial photos for reference of movement.

By 1991, vegetation on the base of the "hook" had increased in density while the beach side towards the Gulf eroded significantly towards the east. From 1994 to 2003, a new sand spit developed eastward at the tip, and further erosion on the Gulf side migrated the entire hook-like mass to the east (Figure 4.6). In 1993, 2 million cubic yards of sand were dredged from the ebb shoal for beach nourishment of the Gulf side of Longboat Key; results of nourishment were still visible on the wider beach zones in 1994 and 2003. Some of the vegetation growth on the south end of Ana Maria key appears to have recessed possibly due to dredging.

Between 2006 and 2009, a further erosion on the Gulf side of Longboat Key's north end was observed, and the new sand spit first observed in 2003 expanded eastward up to the bridge; vegetation also increased in density on the sand spit growing eastward (Figure 4.7).

The trend of eastward migration continued until 2017, with the additional eastward extension beyond the bridge in 2014. Erosion on the Gulf side of Longboat Key's north end accelerated in such way that much of the vegetation present between 1991 and 2009 diminished to the point where it became discontinuous from 2017 until 2020 (Figure 4.8). Manatee County has a $4.9M plan to upgrade the jetty, discussions have been in place since 2017.

In summary, the inlet is extremely active historically, and therefore, lateral channel migration is conservatively assumed to occur throughout the bridge length. All bents will use the current thalweg elevation combined with expected bed degradation as the initial bed elevation applied in local scour calculations.

Figure 4.1 Current Shorelines with 1883 MHW Survey Superimposed (Red Lines)

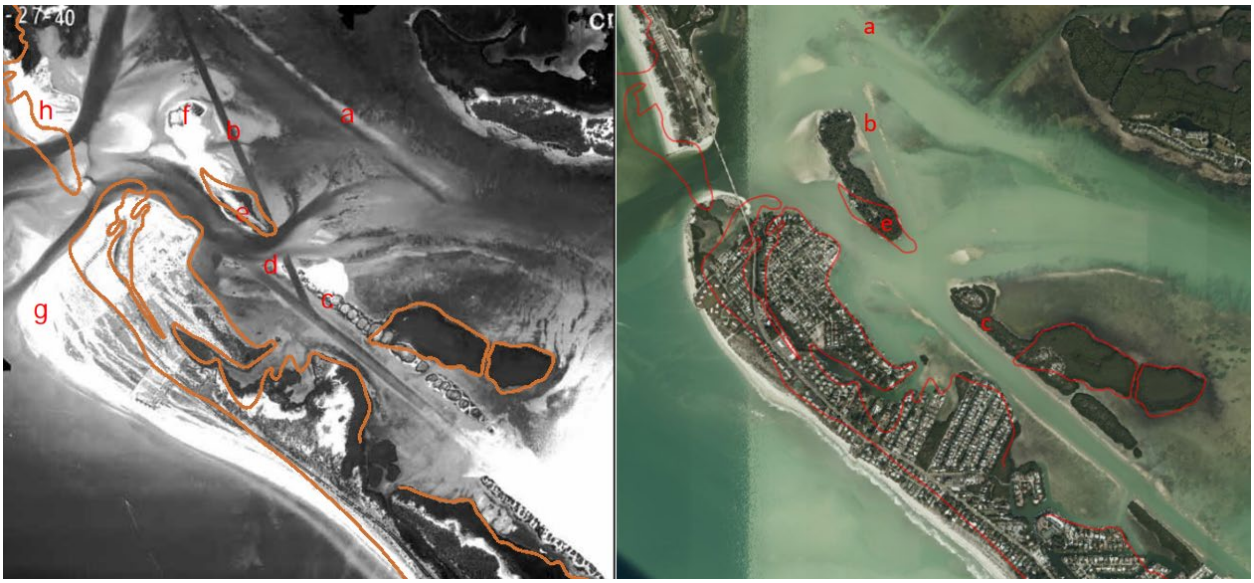

Figure 4.2 Comparison of 1940 (Left) and 2020 (Right) Aerials of Longboat Key with Delineated 1883 Shorelines

Figure 4.3 1952, 1957, and 1962 Aerials of Longboat Inlet

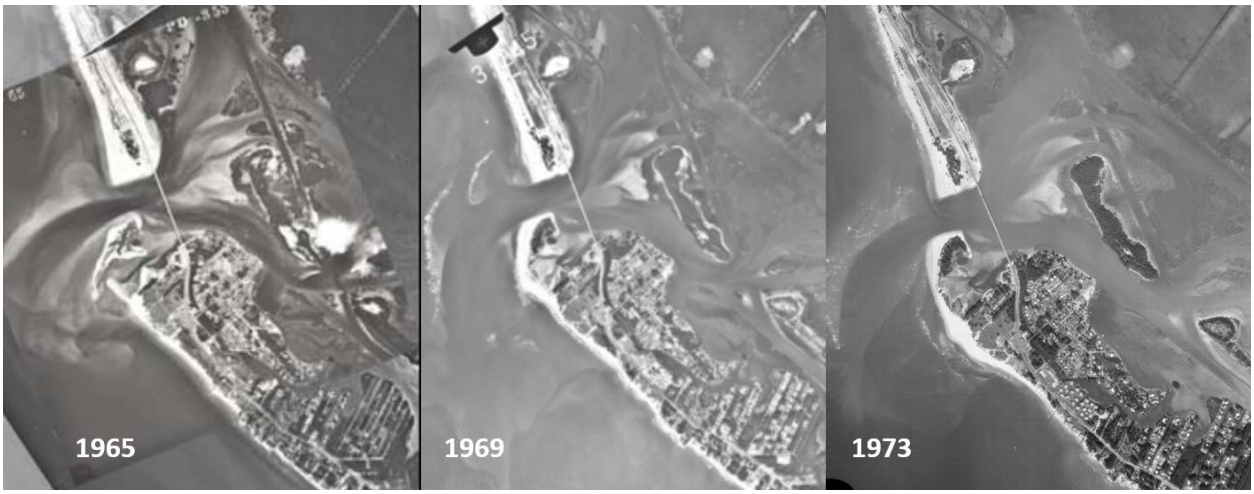

Figure 4.4 1965, 1969, and 1973 Aerials of Longboat Inlet (Source: FDOT)

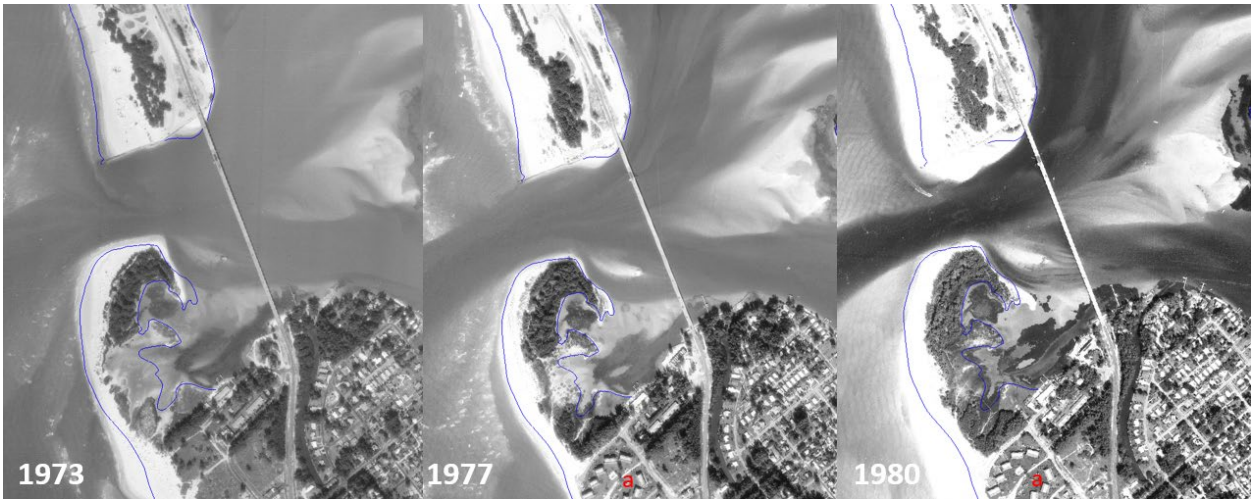

Figure 4.5 1973, 1977, and 1980 Aerials of Longboat Inlet with 1977 Survey Shoreline (blue). (Source: FDOT)

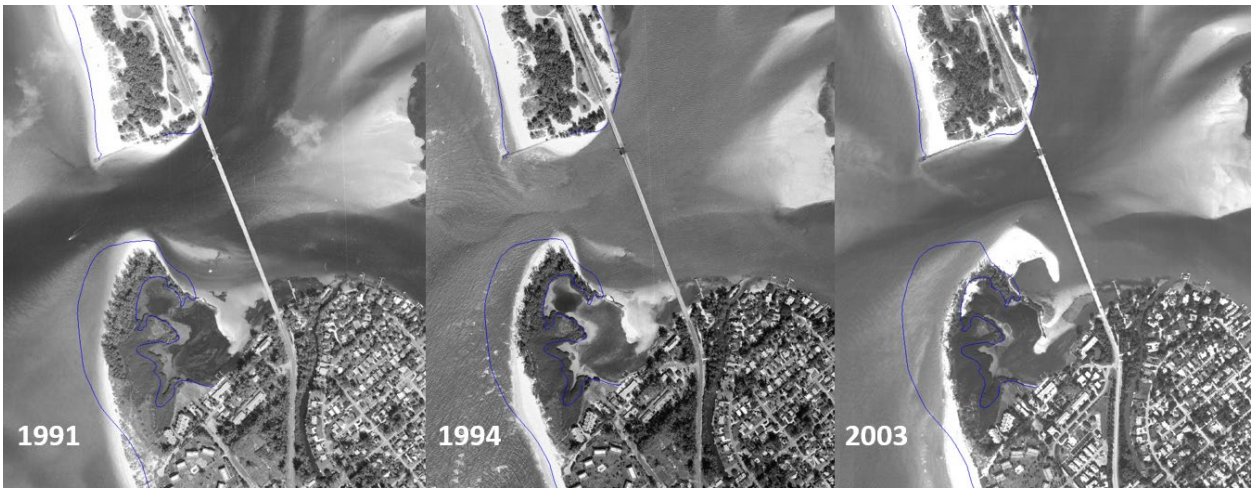

Figure 4.6 1991, 1994, and 2003 Aerials of Longboat Inlet with 1977 Survey Shoreline (blue). (Source: FDOT)

Figure 4.7 2006, 2008, and 2009 Aerials of Longboat Inlet with 1977 Survey Shoreline (blue). (Source: FDOT)

Figure 4.8 2011, 2014, and 2017 Aerials of Longboat Inlet with 1977 Survey Shoreline (blue). (Source: FDOT)

4.2 Contraction Scour

An abrupt decrease in cross-sectional area at a bridge crossing increases flow velocity resulting in contraction scour (a lowering of the channel bottom over the entire width of the channel cross section). Changes in cross-sectional area can result from either natural channel constriction or encroachment of a bridge structure by both the abutments and the piles. HEC-18 presents several equations for contraction scour given various encroachment conditions (cases). The Case 1c (see Figure 4.9) description in HEC-18 (the abutments set back from channel) describes the particular conditions applicable to the bridge. In this case, contraction scour results from the reduction of the flow cross sectional area by the approach embankments, abutments, and piers as the flood event flows through the bridge crossing.

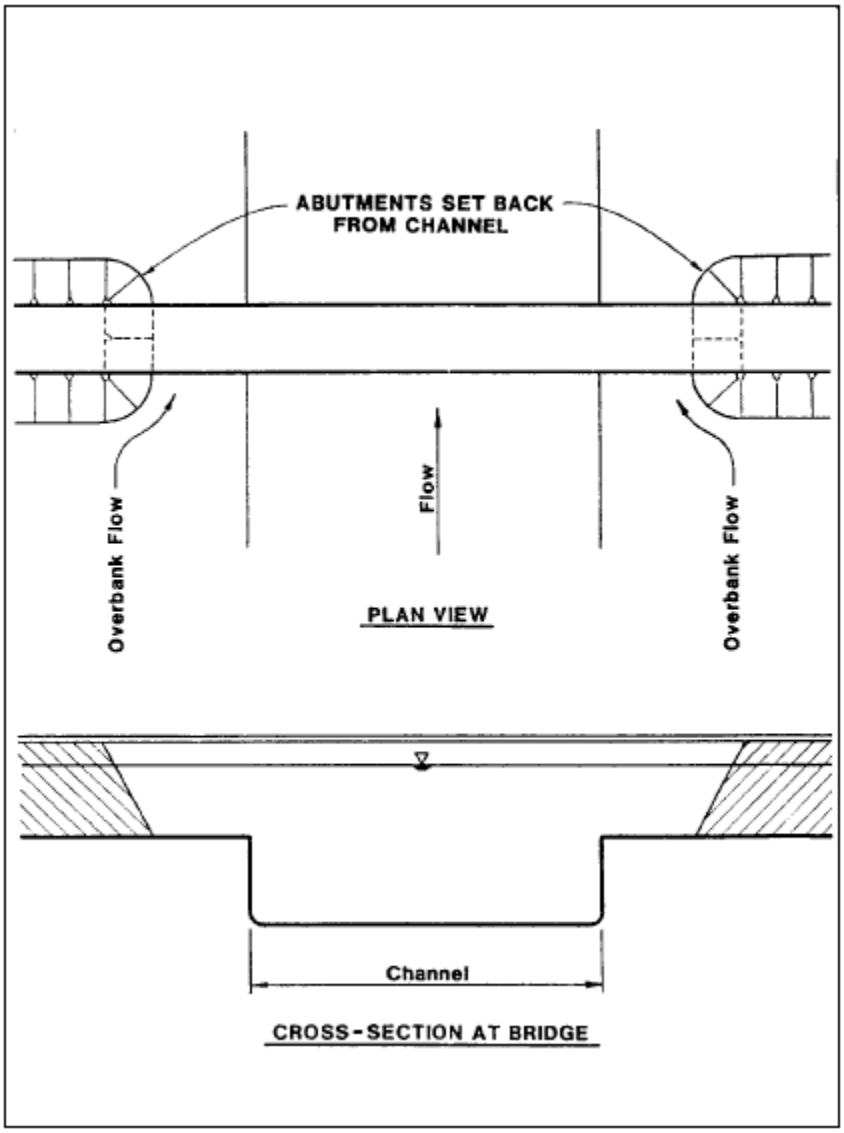

Figure 4.9 Case 1c: Abutments Set Back from Channel (Source: HEC-18)

Computing contraction scour for the bridge requires determining whether the scour is live-bed or clear water. Since the upstream channel velocities exceed the critical velocity for the sediment, the contraction scour is considered live bed for channel. Therefore, contraction scour computations follow the Modified Laursen Live Bed Contraction Scour Equation located in HEC-18 (Section 6.3):

$$\frac{y_2}{y_1} = \left(\frac{Q_2}{Q_1}\right)^{6/7} \left(\frac{W_1}{W_2}\right)^{k_1}$$

where y_1 is the average depth of the upstream cross section, Q_1 and Q_2 are the flow rates through the upstream and downstream cross sections, and W_1 and W_2 are the bottom widths of the upstream and downstream cross sections. k_1 is a constant dependent on the amount of suspended material.

Since the upstream overbank velocity does not exceed the critical velocity for the sediment, the contraction scour is considered clear water for overbanks. Thus, contraction scour computation for the overbank flow follows the Modified Laursen Clear Water Contraction Scour Equation located in HEC-18 (Section 5.3):

$$y_2 = \left[\frac{K_u Q^2}{D_m^{2/3} W^2} \right]^{3/7}$$

where y_2 is the average depth of the contracted section, Q is the flow rate through the cross section, and W is the bottom width of the cross section. D_m is the diameter of the smallest non-transportable particle in the bed material in the contracted section.

The pre-scour average profile depths (y_0) are compared to the post-scour average depths (y_2) to arrive at the contraction scour depths (y_s):

$$y_s = y_2 - y_0.$$

The calculation was conducted using FHWA Hydraulic Toolbox which follows the HEC-18 equations. The inputs and outputs are summarized in Appendix B. The calculations result in similar values for the three alternatives under the 100- and 500-year conditions, i.e., 0 ft for the channel, 4 ft for the left overbank, and 2 ft for the right overbank.

4.3 Local Scour

Local scour refers to bed erosion around obstacles in the path of flow such as bridge piers and abutments. Local scour results from increased shear and normal stresses applied to the bed near the structure due to the presence of the structure. Local pier scour depends on structure geometry, current velocity, angle of attack (the angle between the flow direction and the major axis of the pier/pile group), flow depth, and soil characteristics. Local scour may occur at bridge piers and abutments, but this report only addresses local pier scour since the abutments will have scour protection. This section provides local scour for two hydraulic conditions — the 100-year (design event) and the 500-year (check event).

The local pier scour calculation involved application of the FDOT methodology. The FDOT guidelines for calculating local pier scour require application of the scour equations developed by the FDOT and based on the latest research from the University of Florida for the analysis of complex pier geometries, which includes the equations developed for NCHRP for scour at wide piers (Sheppard et al 2011). This methodology combines the individual scour depths produced by the column, pile cap, and pile group. The local scour is then added to the general and contraction to produce the design scour depths. The FDOT equations predict the scour hole depth based on sediment characteristics, flow parameters, and bent geometry. The flow parameters include depth, velocity, and angle of attack. The bent geometry includes the dimensions of the pile cap and pile group.

As noted in Section 4.1.2, shoreline protection and stabilization measures along the causeway, analysis of historic channel bank lines revealed identifiable lateral bank movement during the record of aerial imagery, and, since no historic bed measurements are available at the site, the thalweg elevation will be applied as the initial bed elevation for the scour analysis. This accounts for possible channel migration during the life of the bridge and is consistent with HEC-18 recommendations.

The local scour was calculated for each bent depending on the bent location: left overbank, channel, and right overbank. Maximum values for velocities, depths, and angle of attack within each region were conservatively applied as local scour calculation inputs. Table 4.1 through Table 4.6 summarize the total scour at each intermediate pier for the 100- and 500-year events. Detailed scour calculations are presented in Appendix C.

Table 4.1 100-Year Scour Calculation Summary for Alternative 1

Bent	Initial Bed Elevation (ft-NAVD88)	Degradation (ft)	Contraction Scour (ft)	Local Scour (ft)	Total Scour (ft)	Final Bed Elevation (ft-NAVD88)
2-7	-26.3	0	2	11.7	13.7	-40
8-12	-26.3	0	0	28.6	28.6	-55
13	-26.3	0	0	69	69	-96
14-15	-26.3	0	0	28.6	28.6	-55
16	-26.3	0	4	9.5	13.5	-40

Table 4.2 500-Year Scour Calculation Summary for Alternative 1

Bent	Initial Bed Elevation (ft-NAVD88)	Degradation (ft)	Contraction Scour (ft)	Local Scour (ft)	Total Scour (ft)	Final Bed Elevation (ft-NAVD88)
2-7	-26.3	0	2	11.8	13.8	-41
8-12	-26.3	0	0	28.9	28.9	-56
13	-26.3	0	0	70.7	70.7	-97
14-15	-26.3	0	0	28.9	28.9	-56
16	-26.3	0	4	10.7	14.7	-41

Table 4.3 100-Year Scour Calculation Summary for Alternative 2

Bent	Initial Bed Elevation (ft-NAVD88)	Degradation (ft)	Contraction Scour (ft)	Local Scour (ft)	Total Scour (ft)	Final Bed Elevation (ft-NAVD88)
2-6	-26.3	0	2	11.7	13.7	-40
7-10	-26.3	0	0	28.6	28.6	-55
11	-26.3	0	0	69	69	-96
12-13	-26.3	0	0	28.6	28.6	-55
14	-26.3	0	4	9.5	13.5	-40

Table 4.4 500-Year Scour Calculation Summary for Alternative 2

Bent	Initial Bed Elevation (ft-NAVD88)	Degradation (ft)	Contraction Scour (ft)	Local Scour (ft)	Total Scour (ft)	Final Bed Elevation (ft-NAVD88)
2-6	-26.3	0	2	11.8	13.8	-41
7-10	-26.3	0	0	28.9	28.9	-56
11	-26.3	0	0	70.7	70.7	-97
12-13	-26.3	0	0	28.9	28.9	-56
14	-26.3	0	4	10.7	14.7	-41

Table 4.5 100-Year Scour Calculation Summary for Alternative 3

Bent	Initial Bed Elevation (ft-NAVD88)	Degradation (ft)	Contraction Scour (ft)	Local Scour (ft)	Total Scour (ft)	Final Bed Elevation (ft-NAVD88)
2-5	-26.3	0	2	11.7	13.7	-40
6-14	-26.3	0	0	28.6	28.6	-55
15-20	-26.3	0	4	9.5	13.5	-40

Table 4.6 500-Year Scour Calculation Summary for Alternative 3

Bent	Initial Bed Elevation (ft-NAVD88)	Degradation (ft)	Contraction Scour (ft)	Local Scour (ft)	Total Scour (ft)	Final Bed Elevation (ft-NAVD88)
2-5	-26.3	0	2	11.8	13.8	-41
6-14	-26.3	0	0	28.9	28.9	-56
15-20	-26.3	0	4	10.7	14.7	-41

5 Other Design Considerations

In addition to flow parameters and scour, the bridge hydraulics report includes design guidance for vertical clearances, sizing riprap protection, and a summary of wave climate.

5.1 Vertical Clearance

The proposed low member elevations are listed in Table 5.1.

Table 5.1 Proposed Low Member Elevations

Alternative	Main Span (ft-NAVD88)	Entire Bridge (ft-NAVD88)
1	+26.06	+14.60
2	+39.06	+16.10
3	+81.06	+19.00

5.1.1 Environment

Structures within the splash zone and with aggressive environments with high chloride content are subject to more corrosive forces. Structure Design Guidelines (FDOT, 2023b) defines the splash zone as the area between 12 ft above MHW and 4 ft below MLW and has additional material requirements to resist corrosion. Given a MHW elevation of +0.34 ft-NAVD88 and SLR of 1.45 ft, the upper limit of the splash zone lies at +13.79 ft-NAVD88. The alternatives all provide the required 12 ft clearance.

5.1.2 Drainage

Section 260.8.1 of FDOT (2023b) specifies a two-foot minimum clearance above the design flood stage for riverine flow. For tidal flow, the FDOT requires the stage associated with the peak velocity through the bridge opening during the design flow. Including SLR, the stage at the bridge during this time equals +8.1 ft NAVD88. The low member elevation of the bridge should lie above +10.1 ft-NAVD88. The alternatives satisfy the drainage clearance criteria.

5.1.3 Navigation

Section 260.8.1 of FDOT (2023b) specifies a six-foot minimum clearance above MHW within the navigation channel of tidal waterbodies. Given an MHW elevation of +0.34 ft-NAVD88 and SLR of 1.45 ft, the low member elevation of the bridge should be at or above +7.79 ft-NAVD88. The alternatives meet the FDOT navigation clearance criteria.

USCG (United States Coast Guard) requires minimum horizontal and vertical clearances for the navigational span. The required minimum clearances for the three alternatives are listed Table 5.2 The alternatives meet the USCG navigation clearance criteria.

Table 5.2 USCG Required Minimum Navigation Clearance

Alternative	Min. Horizontal Clearance (ft)	Proposed Horizontal Clearance (ft)	Min. Vertical Clearance (ft)	Required Elevation (ft-NAVD88)	Proposed Elevation (ft-NAVD88)
1	90	175	23	+24.79	+26.06
2	90	175	36	+37.79	+39.06
3	100	155	78	+79.79	+81.06

5.1.4 Coastal Bridges

Given the bridges' location, wind-generated (hurricane-generated) waves could reach the bridge during a design hurricane landfall event. For coastal bridges, Section 260.8.1 of FDOT (2023b) stipulates that the vertical clearance of the superstructure must lie at least one foot above the 100-yr wave crest elevation.

Following the AASHTO code (AASHTO, 2008), the maximum wave height equals 1.8 times the significant wave height. However, water depth and wave steepness limit maximum wave heights achievable. As such, the AASHTO code recommends taking the lesser of 1.8 times the significant wave height, depth-limited wave height, and steepness-limited wave height as the maximum wave height (*Hmax*). Wave crest elevation calculations assumed that 70% of the maximum wave height lies above the still water level (maximum storm surge water surface elevation at the bridges).

The wave crest elevation reaches +15.1 ft-NAVD88 (+13.6 ft-NAVD88 without SLR), the low member elevation of the bridge should be at or above +16.1 ft-NAVD88. Therefore, alternatives 2 and 3 satisfy the wave crest clearance.

It is worth noting that, span 1 of alternative 1 partially encroaches on the 1 ft clearance above the 100-year design wave crest elevation adjusted for sea level rise of 15.1 ft at the south end of the span near end bent 1. Nevertheless, this is not a concern as the wave height (Hs = 3.8 ft) contributing to the +15.1 ft-NAVD88 was obtained from the center of the channel; while the wave height near span 1 is smaller (Hs = 1.3 ft), resulting a wave crest elevation of approximately 12.0 ft-NAVD88. Therefore, a wave force calculation is not needed.

5.2 Abutment Protection

Design flow velocities through the bridge opening (6.6 fps) lie below the allowable limit (7.2 fps) for FDOT Standard Bank and Shore Rubble Riprap (530-2.2.1). The modified Isbash equation provides the methodology for sizing armor stone under design currents. Employing the conditions from the 100-year simulations, the equation yields a median stone weight of 0.3 lbs (0.2 ft.). Application of the van der Meer's methodology for sizing a riprap yielded a median stone weight of 329 lbs (1.25 ft). Based on the results of these two calculations, FDOT Standard Bank and Shore Rubble Riprap (530-2.2.1) provides stable scour protection for the abutments. The riprap shall be at least two stone diameters (2.5 ft) thick, and underlaid by bedding stone (1.0 ft thick) and an FDOT approved geotextile filter fabric. According to FDOT Drainage Manual Section 4.9.1, abutment protection must have a horizontal toe berm extending 10 ft beyond the toe of the abutment slope. This protection will protect the slope above the bulkhead and be placed at a slope steepness of no greater than 2:1 (H:V). The riprap berm at the bulkhead toe must extend at least 10 ft from the bulkhead. The protection should wrap the abutments and tie back into the existing riprap protecting the causeway. Details of the armor stone size calculations are included in Appendix E.

6 References

Arneson, L. A., Zevenbergen, L. W., Lagasse, P. F., and Clopper, P. E. (2012). *Evaluating Scour at Bridges. Fifth Edition. Federal Highway Administration, Hydraulic Engineering Circular No. 18 (HEC-18).* US Department of Transportation. FHWA, Washington DC.

Federal Emergency Management Agency. (2021). Effective Flood Insurance Study, Manatee County, Florida, and Incorporated Areas.

Florida Department of Transportation. (2023). Drainage Manual. Florida Department of Transportation. Tallahassee: FDOT.

Florida Department of Transportation (2023). Drainage Design Guide. Florida Department of Transportation. Tallahassee: FDOT.

Florida Department of Transportation. (2023). FDOT Design Manual. Florida Department of Transportation. Tallahassee: FDOT.

P.F. Lagasse, L.W. Zevenbergen, W.J. Spitz, L.A. Arneson (2012). Stream Stability at Highway Structures.
Fourth Edition. Federal Highway Administration, Hydraulic Engineering Circular No. 20 (HEC-20). US Department of Transportation. FHWA, Washington DC.

Florida Department of Transportation (2022). Florida Bridge Scour Manual. Florida Department of Transportation. Tallahassee: FDOT.

US Army Corps of Engineers (2002). *Coastal Engineering Manual.* EM 1110-2-1100. US Army Corps of Engineers. Washington, DC.

Appendix A – Historic Aerial Imagery

Figure A. 1 2017 Aerial Photograph (Source: FDOT)

Figure A. 2 2014 Aerial Photograph (Source: FDOT)

Figure A. 3 2011 Aerial Photograph (Source: FDOT)

Figure A. 4 2009 Aerial Photograph (Source: FDOT)

Figure A. 5 2008 Aerial Photograph (Source: FDOT)

Figure A. 6 2006 Aerial Photograph (Source: FDOT)

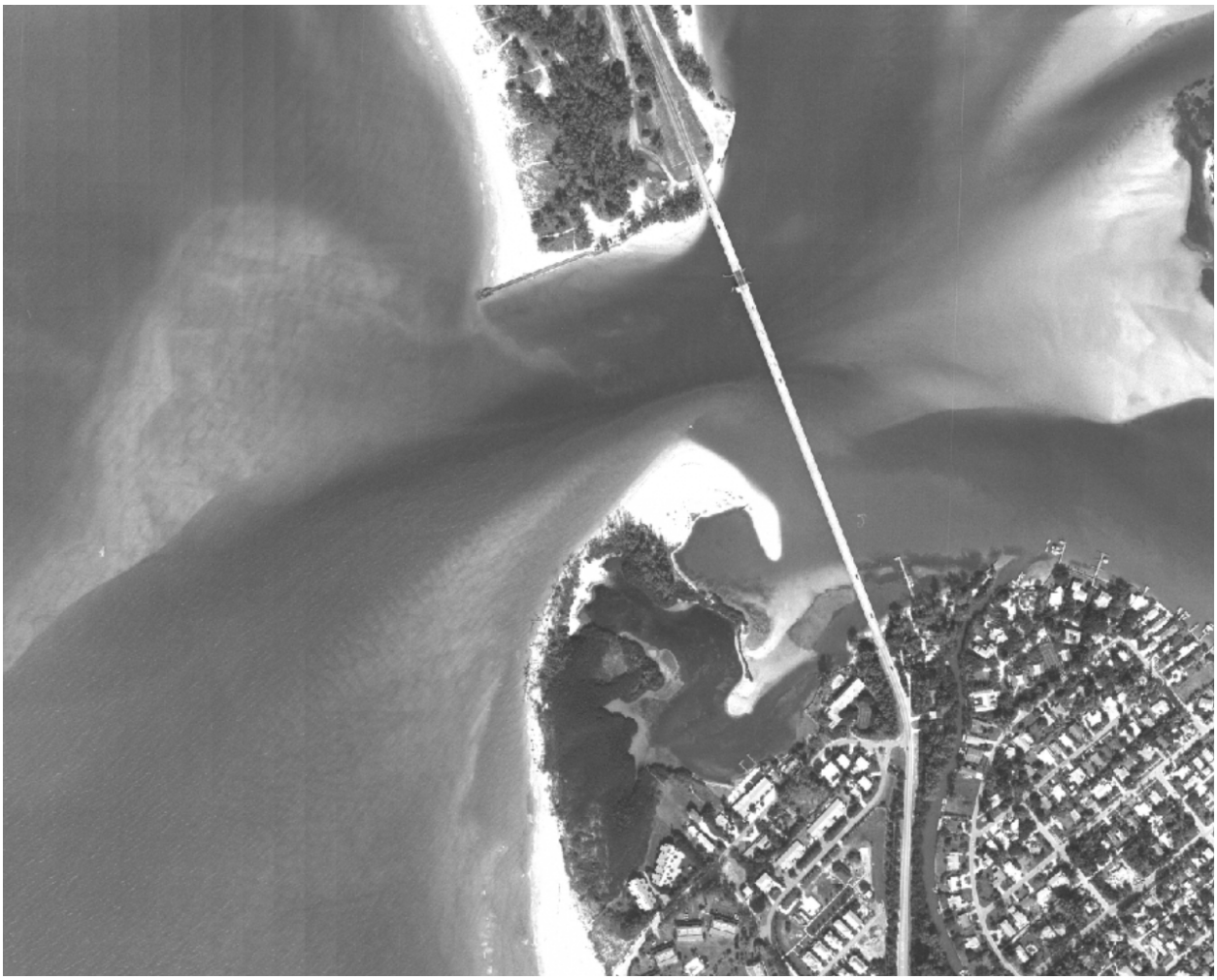

Figure A. 7 2003 Aerial Photograph (Source: FDOT)

Figure A. 8 1994 Aerial Photograph (Source: FDOT)

Figure A. 9 1991 Aerial Photograph (Source: FDOT)

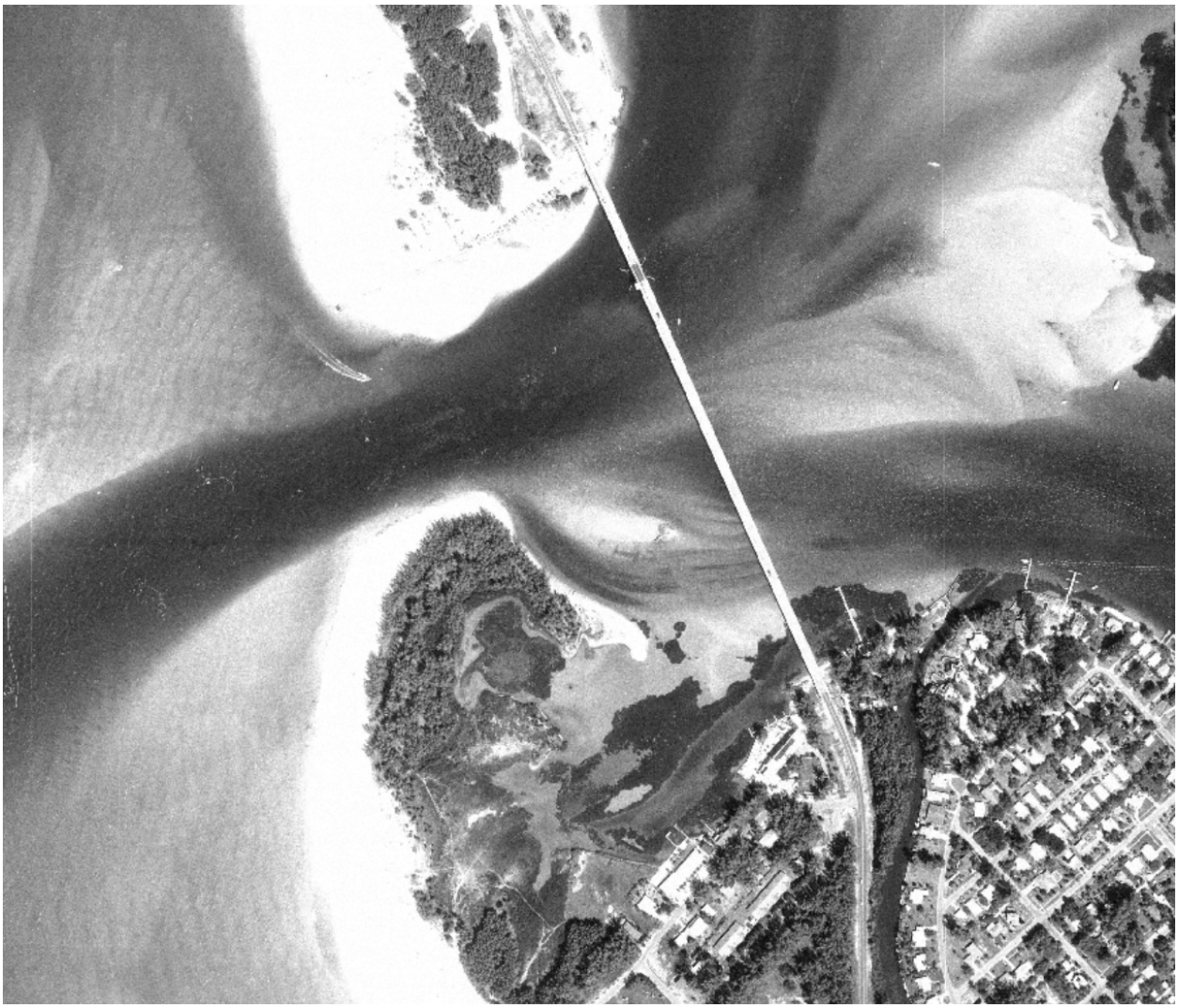

Figure A. 10 1980 Aerial Photograph (Source: FDOT)

Figure A. 11 1977 Aerial Photograph (Source: FDOT)

Figure A. 12 1973 Aerial Photograph (Source: FDOT)

Figure A. 13 1969 Aerial Photograph (Source: Dabees, et. al., 2008)

Figure A. 14 1965 Aerial Photograph (Source: Dabees, et. al., 2008)

Figure A. 15 1962 Aerial Photograph (Source: Dabees, et. al., 2008)

Appendix B – Contraction Scour Calculations

Alternative 1

100-year

Channel

Contraction Scour

Computation Method: Clear-Water or Live-Bed Scour

Parameter	Value	Units	Notes
Input Parameters			
Average Depth Upstream of Contraction	16.60	ft	
D50	0.200000	mm	0.2 mm is the lower li...
Average Velocity Upstream	6.60	ft/s	
Results of Scour Condition			
Critical velocity above which bed material of siz...	1.55	ft/s	
Contraction Scour Condition	Live Bed		
Live Bed Input Parameters			
Temperature of Water	60.00	ºF	
Slope of Energy Grade Line at Approach Section	0.000010	ft/ft	
Discharge in Contracted Section	207926.00	cfs	
Discharge Upstream that is Transporting Sediment	197878.00	cfs	
Width in Contracted Section	1077.00	ft	Remove widths occupie...
Width Upstream that is Transporting Sediment	1610.00	ft	
Depth Prior to Scour in Contracted Section	24.00	ft	
Unit Weight of Water	62.40	lb/ft^3	
Unit Weight of Sediment	165.00	lb/ft^3	
Results			
k1	0.640000		
Shear Velocity	0.07	ft/s	
Fall Velocity	0.08	ft/s	
Average Depth in Contracted Section after Scour	22.40	ft	
Scour Depth	-1.60	ft	Negative values imply '...

Left overbank

Contraction Scour

Computation Method: Clear-Water or Live-Bed Scour

Parameter	Value	Units	Notes
Input Parameters			
Average Depth Upstream of Contraction	7.00	ft	
D50	0.200000	mm	0.2 mm is the lower li...
Average Velocity Upstream	1.20	ft/s	
Results of Scour Condition			
Critical velocity above which bed material of siz...	1.34	ft/s	
Contraction Scour Condition	Clear Water		
Clear Water Input Parameters			
Discharge in Contracted Section	12062.00	cfs	
Bottom Width in Contracted Section	702.00	ft	Width should exclude p...
Depth Prior to Scour in Contracted Section	7.00	ft	
Results			
Diameter of the smallest nontransportable partic...	0.250000	mm	
Average Depth in Contracted Section after Scour	10.83	ft	
Scour Depth	3.83	ft	Negative values imply '...

Right overbank

Contraction Scour

Computation Method: Clear-Water or Live-Bed Scour

Parameter	Value	Units	Notes
Input Parameters			
Average Depth Upstream of Contraction	13.60	ft	
D50	0.200000	mm	0.2 mm is the lower li...
Average Velocity Upstream	1.40	ft/s	
Results of Scour Condition			
Critical velocity above which bed material of siz...	1.50	ft/s	
Contraction Scour Condition	Clear Water		
Clear Water Input Parameters			
Discharge in Contracted Section	2485.00	cfs	
Bottom Width in Contracted Section	212.00	ft	Width should exclude p...
Depth Prior to Scour in Contracted Section	7.00	ft	
Results			
Diameter of the smallest nontransportable partic...	0.250000	mm	
Average Depth in Contracted Section after Scour	7.80	ft	
Scour Depth	0.80	ft	Negative values imply '...

500-year

Channel

Contraction Scour

Computation Method: Clear-Water or Live-Bed Scour

Parameter	Value	Units	Notes
Input Parameters			
Average Depth Upstream of Contraction	18.00	ft	
D50	0.200000	mm	0.2 mm is the lower li...
Average Velocity Upstream	5.70	ft/s	
Results of Scour Condition			
Critical velocity above which bed material of siz...	1.57	ft/s	
Contraction Scour Condition	Live Bed		
Live Bed Input Parameters			
Temperature of Water	60.00	ºF	
Slope of Energy Grade Line at Approach Section	0.000010	ft/ft	
Discharge in Contracted Section	193609.00	cfs	
Discharge Upstream that is Transporting Sediment	183606.00	cfs	
Width in Contracted Section	1077.00	ft	Remove widths occupie...
Width Upstream that is Transporting Sediment	1610.00	ft	
Depth Prior to Scour in Contracted Section	25.60	ft	
Unit Weight of Water	62.40	lb/ft^3	
Unit Weight of Sediment	165.00	lb/ft^3	
Results			
k1	0.640000		
Shear Velocity	0.08	ft/s	
Fall Velocity	0.08	ft/s	
Average Depth in Contracted Section after Scour	24.37	ft	
Scour Depth	-1.23	ft	Negative values imply '...

Left overbank

Contraction Scour

Computation Method: Clear-Water or Live-Bed Scour

Parameter	Value	Units	Notes
Input Parameters			
Average Depth Upstream of Contraction	10.00	ft	
D50	0.200000	mm	0.2 mm is the lower li...
Average Velocity Upstream	1.30	ft/s	
Results of Scour Condition			
Critical velocity above which bed material of siz...	1.42	ft/s	
Contraction Scour Condition	Clear Water		
Clear Water Input Parameters			
Discharge in Contracted Section	14199.00	cfs	
Bottom Width in Contracted Section	702.00	ft	Width should exclude p...
Depth Prior to Scour in Contracted Section	10.00	ft	
Results			
Diameter of the smallest nontransportable partic...	0.250000	mm	
Average Depth in Contracted Section after Scour	12.45	ft	
Scour Depth	2.45	ft	Negative values imply '...

Right overbank

Contraction Scour

Computation Method: Clear-Water or Live-Bed Scour

Parameter	Value	Units	Notes
Input Parameters			
Average Depth Upstream of Contraction	10.00	ft	
D50	0.200000	mm	0.2 mm is the lower li...
Average Velocity Upstream	1.30	ft/s	
Results of Scour Condition			
Critical velocity above which bed material of siz...	1.42	ft/s	
Contraction Scour Condition	Clear Water		
Clear Water Input Parameters			
Discharge in Contracted Section	2485.00	cfs	
Bottom Width in Contracted Section	212.00	ft	Width should exclude p...
Depth Prior to Scour in Contracted Section	10.00	ft	
Results			
Diameter of the smallest nontransportable partic...	0.250000	mm	
Average Depth in Contracted Section after Scour	7.80	ft	
Scour Depth	-2.20	ft	Negative values imply '...

Alternative 2

100-year

Channel

Contraction Scour

Computation Method: Clear-Water or Live-Bed Scour

Parameter	Value	Units	Notes
Input Parameters			
Average Depth Upstream of Contraction	16.60	ft	
D50	0.200000	mm	0.2 mm is the lower li...
Average Velocity Upstream	6.60	ft/s	
Results of Scour Condition			
Critical velocity above which bed material of siz...	1.55	ft/s	
Contraction Scour Condition	Live Bed		
Live Bed Input Parameters			
Temperature of Water	60.00	ºF	
Slope of Energy Grade Line at Approach Section	0.000010	ft/ft	
Discharge in Contracted Section	207926.00	cfs	
Discharge Upstream that is Transporting Sediment	197878.00	cfs	
Width in Contracted Section	1077.00	ft	Remove widths occupie...
Width Upstream that is Transporting Sediment	1610.00	ft	
Depth Prior to Scour in Contracted Section	24.00	ft	
Unit Weight of Water	62.40	lb/ft^3	
Unit Weight of Sediment	165.00	lb/ft^3	
Results			
k1	0.640000		
Shear Velocity	0.07	ft/s	
Fall Velocity	0.08	ft/s	
Average Depth in Contracted Section after Scour	22.40	ft	
Scour Depth	-1.60	ft	Negative values imply '...

Left overbank

Contraction Scour

Computation Method: Clear-Water or Live-Bed Scour

Parameter	Value	Units	Notes
Input Parameters			
Average Depth Upstream of Contraction	7.00	ft	
D50	0.200000	mm	0.2 mm is the lower li...
Average Velocity Upstream	1.20	ft/s	
Results of Scour Condition			
Critical velocity above which bed material of siz...	1.34	ft/s	
Contraction Scour Condition	Clear Water		
Clear Water Input Parameters			
Discharge in Contracted Section	12062.00	cfs	
Bottom Width in Contracted Section	710.00	ft	Width should exclude p...
Depth Prior to Scour in Contracted Section	7.00	ft	
Results			
Diameter of the smallest nontransportable partic...	0.250000	mm	
Average Depth in Contracted Section after Scour	10.72	ft	
Scour Depth	3.72	ft	Negative values imply '...

Right overbank

Contraction Scour

Computation Method: Clear-Water or Live-Bed Scour

Parameter	Value	Units	Notes
Input Parameters			
Average Depth Upstream of Contraction	13.60	ft	
D50	0.200000	mm	0.2 mm is the lower li...
Average Velocity Upstream	1.40	ft/s	
Results of Scour Condition			
Critical velocity above which bed material of siz...	1.50	ft/s	
Contraction Scour Condition	Clear Water		
Clear Water Input Parameters			
Discharge in Contracted Section	2485.00	cfs	
Bottom Width in Contracted Section	204.00	ft	Width should exclude p...
Depth Prior to Scour in Contracted Section	7.00	ft	
Results			
Diameter of the smallest nontransportable partic...	0.250000	mm	
Average Depth in Contracted Section after Scour	8.06	ft	
Scour Depth	1.06	ft	Negative values imply '...

500-year

Channel

Contraction Scour

Computation Method: Clear-Water or Live-Bed Scour

Parameter	Value	Units	Notes
Input Parameters			
Average Depth Upstream of Contraction	18.00	ft	
D50	0.200000	mm	0.2 mm is the lower li...
Average Velocity Upstream	5.70	ft/s	
Results of Scour Condition			
Critical velocity above which bed material of siz...	1.57	ft/s	
Contraction Scour Condition	Live Bed		
Live Bed Input Parameters			
Temperature of Water	60.00	ºF	
Slope of Energy Grade Line at Approach Section	0.000010	ft/ft	
Discharge in Contracted Section	193609.00	cfs	
Discharge Upstream that is Transporting Sediment	183606.00	cfs	
Width in Contracted Section	1077.00	ft	Remove widths occupie...
Width Upstream that is Transporting Sediment	1610.00	ft	
Depth Prior to Scour in Contracted Section	25.60	ft	
Unit Weight of Water	62.40	lb/ft^3	
Unit Weight of Sediment	165.00	lb/ft^3	
Results			
k1	0.640000		
Shear Velocity	0.08	ft/s	
Fall Velocity	0.08	ft/s	
Average Depth in Contracted Section after Scour	24.37	ft	
Scour Depth	-1.23	ft	Negative values imply '...

Left overbank

Contraction Scour

Computation Method: Clear-Water or Live-Bed Scour

Parameter	Value	Units	Notes
Input Parameters			
Average Depth Upstream of Contraction	10.00	ft	
D50	0.200000	mm	0.2 mm is the lower li...
Average Velocity Upstream	1.30	ft/s	
Results of Scour Condition			
Critical velocity above which bed material of siz...	1.42	ft/s	
Contraction Scour Condition	Clear Water		
Clear Water Input Parameters			
Discharge in Contracted Section	14199.00	cfs	
Bottom Width in Contracted Section	710.00	ft	Width should exclude p...
Depth Prior to Scour in Contracted Section	10.00	ft	
Results			
Diameter of the smallest nontransportable partic...	0.250000	mm	
Average Depth in Contracted Section after Scour	12.33	ft	
Scour Depth	2.33	ft	Negative values imply '...

Right overbank

Contraction Scour

Computation Method: Clear-Water or Live-Bed Scour

Parameter	Value	Units	Notes
Input Parameters			
Average Depth Upstream of Contraction	10.00	ft	
D50	0.200000	mm	0.2 mm is the lower li...
Average Velocity Upstream	1.30	ft/s	
Results of Scour Condition			
Critical velocity above which bed material of siz...	1.42	ft/s	
Contraction Scour Condition	Clear Water		
Clear Water Input Parameters			
Discharge in Contracted Section	2485.00	cfs	
Bottom Width in Contracted Section	204.00	ft	Width should exclude p...
Depth Prior to Scour in Contracted Section	10.00	ft	
Results			
Diameter of the smallest nontransportable partic...	0.250000	mm	
Average Depth in Contracted Section after Scour	8.06	ft	
Scour Depth	-1.94	ft	Negative values imply '...

Alternative 3

100-year

Channel

Contraction Scour

Computation Method: Clear-Water or Live-Bed Scour

Parameter	Value	Units	Notes
Input Parameters			
Average Depth Upstream of Contraction	16.60	ft	
D50	0.200000	mm	0.2 mm is the lower li...
Average Velocity Upstream	6.60	ft/s	
Results of Scour Condition			
Critical velocity above which bed material of siz...	1.55	ft/s	
Contraction Scour Condition	Live Bed		
Live Bed Input Parameters			
Temperature of Water	60.00	ºF	
Slope of Energy Grade Line at Approach Section	0.000010	ft/ft	
Discharge in Contracted Section	207926.00	cfs	
Discharge Upstream that is Transporting Sediment	197878.00	cfs	
Width in Contracted Section	1126.00	ft	Remove widths occupie...
Width Upstream that is Transporting Sediment	1610.00	ft	
Depth Prior to Scour in Contracted Section	24.00	ft	
Unit Weight of Water	62.40	lb/ft^3	
Unit Weight of Sediment	165.00	lb/ft^3	
Results			
k1	0.640000		
Shear Velocity	0.07	ft/s	
Fall Velocity	0.08	ft/s	
Average Depth in Contracted Section after Scour	21.77	ft	
Scour Depth	-2.23	ft	Negative values imply '...

Left overbank

Contraction Scour

Computation Method: Clear-Water or Live-Bed Scour

Parameter	Value	Units	Notes
Input Parameters			
Average Depth Upstream of Contraction	7.00	ft	
D50	0.200000	mm	0.2 mm is the lower li...
Average Velocity Upstream	1.20	ft/s	
Results of Scour Condition			
Critical velocity above which bed material of siz...	1.34	ft/s	
Contraction Scour Condition	Clear Water		
Clear Water Input Parameters			
Discharge in Contracted Section	12062.00	cfs	
Bottom Width in Contracted Section	718.00	ft	Width should exclude p...
Depth Prior to Scour in Contracted Section	7.00	ft	
Results			
Diameter of the smallest nontransportable partic...	0.250000	mm	
Average Depth in Contracted Section after Scour	10.62	ft	
Scour Depth	3.62	ft	Negative values imply '...

Right overbank

Contraction Scour

Computation Method: Clear-Water or Live-Bed Scour

Parameter	Value	Units	Notes
Input Parameters			
Average Depth Upstream of Contraction	13.60	ft	
D50	0.200000	mm	0.2 mm is the lower li...
Average Velocity Upstream	1.40	ft/s	
Results of Scour Condition			
Critical velocity above which bed material of siz...	1.50	ft/s	
Contraction Scour Condition	Clear Water		
Clear Water Input Parameters			
Discharge in Contracted Section	10387.00	cfs	
Bottom Width in Contracted Section	1104.00	ft	Width should exclude p...
Depth Prior to Scour in Contracted Section	6.00	ft	
Results			
Diameter of the smallest nontransportable partic...	0.250000	mm	
Average Depth in Contracted Section after Scour	6.46	ft	
Scour Depth	0.46	ft	Negative values imply '...

500-year

Channel

Contraction Scour

Computation Method: Clear-Water or Live-Bed Scour

Parameter	Value	Units	Notes
Input Parameters			
Average Depth Upstream of Contraction	18.00	ft	
D50	0.200000	mm	0.2 mm is the lower li...
Average Velocity Upstream	5.70	ft/s	
Results of Scour Condition			
Critical velocity above which bed material of siz...	1.57	ft/s	
Contraction Scour Condition	Live Bed		
Live Bed Input Parameters			
Temperature of Water	60.00	ºF	
Slope of Energy Grade Line at Approach Section	0.000010	ft/ft	
Discharge in Contracted Section	193609.00	cfs	
Discharge Upstream that is Transporting Sediment	183606.00	cfs	
Width in Contracted Section	1126.00	ft	Remove widths occupie...
Width Upstream that is Transporting Sediment	1610.00	ft	
Depth Prior to Scour in Contracted Section	25.60	ft	
Unit Weight of Water	62.40	lb/ft^3	
Unit Weight of Sediment	165.00	lb/ft^3	
Results			
k1	0.640000		
Shear Velocity	0.08	ft/s	
Fall Velocity	0.08	ft/s	
Average Depth in Contracted Section after Scour	23.68	ft	
Scour Depth	-1.92	ft	Negative values imply '...

Left overbank

Contraction Scour

Computation Method: Clear-Water or Live-Bed Scour

Parameter	Value	Units	Notes
Input Parameters			
Average Depth Upstream of Contraction	10.00	ft	
D50	0.200000	mm	0.2 mm is the lower li...
Average Velocity Upstream	1.30	ft/s	
Results of Scour Condition			
Critical velocity above which bed material of siz...	1.42	ft/s	
Contraction Scour Condition	Clear Water		
Clear Water Input Parameters			
Discharge in Contracted Section	14199.00	cfs	
Bottom Width in Contracted Section	718.00	ft	Width should exclude p...
Depth Prior to Scour in Contracted Section	10.00	ft	
Results			
Diameter of the smallest nontransportable partic...	0.250000	mm	
Average Depth in Contracted Section after Scour	12.22	ft	
Scour Depth	2.22	ft	Negative values imply '...

Right overbank

Contraction Scour

Computation Method: Clear-Water or Live-Bed Scour

Parameter	Value	Units	Notes
Input Parameters			
Average Depth Upstream of Contraction	15.70	ft	
D50	0.200000	mm	0.2 mm is the lower li...
Average Velocity Upstream	1.40	ft/s	
Results of Scour Condition			
Critical velocity above which bed material of siz...	1.54	ft/s	
Contraction Scour Condition	Clear Water		
Clear Water Input Parameters			
Discharge in Contracted Section	28445.00	cfs	
Bottom Width in Contracted Section	1104.00	ft	Width should exclude p...
Depth Prior to Scour in Contracted Section	14.00	ft	
Results			
Diameter of the smallest nontransportable partic...	0.250000	mm	
Average Depth in Contracted Section after Scour	15.33	ft	
Scour Depth	1.33	ft	Negative values imply '...

Appendix C – Local Scour Calculations

Appendix D – Field Review Photos

Figure F. 1 Bulkhead and riprap toe protection northeast of bridge

Figure F. 2 Northeast abutment

Figure F. 3 East bridge face

Figure F. 4 Bulkhead and riprap toe protection near north end of bridge

Figure F. 5 Northwest Abutment

Figure F. 6 Bridge Number

Figure F. 7 Longboat Pass as viewed from north end of bridge

Figure F. 8 West bridge face as viewed from near northwest abutment

Figure F. 9 West Bridge Face

Figure F. 10 Derelict pier west of bridge

Figure F. 11 West bridge face

Figure F. 12 Longboat pass west of bridge as viewed from north shoreline

Figure F. 13 Geotube beach stabilization near derelict pier

Figure F. 14 South abutment slope

Figure F. 15 West face of bridge over lagoon

Figure F. 16 East face of bridge over lagoon

Figure F. 17 East face of bridge as viewed from southeast

Figure F. 18 Area east of bridge between Longboat Pass and lagoon

Figure F. 19 Lagoon west of bridge

Figure F. 20 Lagoon west of bridge

Figure F. 21 Lagoon east of bridge

Figure F. 22 Longboat Pass east of bridge

Appendix E – Armor Stone Size Calculations

Armor Stone Size Calculation (flow velocity): Isbash HEC-23

HEC-23 (Lagasse et al., 2009) (2 14-1)			
Input			
avg. channel flow depth		7	ft
contracted section velocity	V	4	ft/s
contracted section depth	y	7	ft
Unit weight of stone	w_a	165	lbs/ft^3
Unit weight of water	w_w	62.4	lbs/ft^3
abutment type		spill-through	
Safety Factor on Velocicity	SF	2	
Intermediate			
Froude No. $[V/(gy)^{0.5}]$		0.26643	
	K	0.89	
spec gravity		2.644231	
	$D = r_s/r-1$	1.644231	
	yK/D	3.789006	
Output			
	D_{50}	0.153693	ft
		1.844313	in
	W_{50}	0.313648	lbs

Armor Stone Calculation (waves): van der Meer (1988)

Armor Stone Calculation Using van der Meer (1988)		
Non-Overtopped Slopes		
Input		
cot a	2.0	
H_s*	1.4	m
T_p	4.5	s
P	0.5	
r_s	2650	kg/m^3
r_w	1020	kg/m^3
N	1000	
g	9.81	m/s^2
T_p/T_m	1.25	
S_d	2	
Intermediate		
T_m	3.6	s
L_o	20	m
a	0.031	
H_{sc}	0.4	m
D	1.60	
K_{pl}	22.39	
K_{su}	0.35	
Output		
H_s	*is greater than*	H_{sc}
Therefore,	*Plunging waves*	
Plunging		
M_{50}	149	kg
	329	lbs
	0.2	tons (U.S)
D_{50}	0.4	m
	1.25	ft
Surging		
M_{50}	961.3	kg
	2119.37	lbs
	1.1	tons (U.S)
D_{50}	0.71	m
	2.3	ft

* The north bank can be directly attacked by waves while the south bank is sheltered by vegetations. The significant wave height is 2 ft at the north bank and 1.3 ft at the south bank. The average water depth of the north bank is about 5.8 ft during the 100-year storm, resulting a depth-limited wave height of 4.6 ft. This is significantly greater than 2 ft, therefore was conservatively used in the calculation.